Fuel 326 (2022) 125124

Contents lists available at ScienceDirect

Fuel

journal homepage: www.elsevier.com/locate/fuel

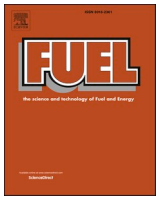

Review article

A critical review of coal permeability models

Qi Gao [a,*], Jishan Liu [a], Yifan Huang [a], Wai Li [a], Rui Shi [b], Yee-Kwong Leong [a], Derek Elsworth [c]

[a] School of Engineering, The University of Western Australia, Perth, WA 6009, Australia
[b] School of Resources and Geosciences, China University of Mining and Technology, Xuzhou 221116, China
[c] Department of Energy and Mineral Engineering, G3 Centre and Energy Institute, The Pennsylvania State University, University Park, PA 16802, USA

ARTICLE INFO

Keywords:
Coal permeability model
Internal structure
Boundary condition
Equilibrium state

ABSTRACT

The evolution of coal permeability is very complex under the influence of coupled multiple processes. This is the primary motivation why numerous coal permeability models have been developed over the last decades. Although great efforts have been made to evaluate these models, the root causes of discrepancies between lab/field observations and model predictions are still not identified. The objectives of this study are to address this problem from the perspective of model selves and explore their implications for further improvements. In this study, we collected all coal permeability models available in the literature. Through analysis, we conclude that all models can be characterized by a combination of internal structure of coal, boundary conditions and equilibrium state within the controlled volume. Different combinations lead to two major categories of coal permeability models. One category is structure-based equilibrium models including matchstick, cubic and rock bridge models. The other category is structure-based non-equilibrium models. The equilibrium models only serve as the upper and lower envelopes of experimental data while the non-equilibrium models can explain the data in-between. Further analysis concludes that if local equilibrium is achieved, gas pressure and its associated swelling strain distribute uniformly throughout the entire volume and that if not achieved, both pressure and swelling strain distribute non-uniformly. These conclusions suggest that the exclusion of equilibration process between fracture and matrix systems is the root cause of discrepancies between lab/field observations and model predictions and that future research work should integrate rock structure, boundary conditions and equilibration process in coal permeability model. This inclusion of transient process within the controlled volume represents a leap of knowledge from equilibrium to non-equilibrium theory and opens up a new realm for unconventional gas reservoir modelling.

1. Introduction

Naturally fractured coal is typically treated as a dual porosity medium with porous matrixes isolated by intersecting cleats (also called fractures). The porous matrix blocks provide the main storage site for around 95% of total gas in place as the micropores in it have the extremely large internal surface area with strong affinity to methane [1,2]. The remaining gas is stored in the macropores, i.e., cleats. The cleat system can be subdivided into two groups [3]. One group is called face cleats which are continuous and well-developed across the reservoir. The other group is called butt cleats which are discontinuous and usually terminate at the intersections with face cleats. Due to the heterogeneous pore systems, gas transport mechanisms in coal seams are substantially different from that of the conventional gas reservoirs [4,5]. As shown in Fig. 1, three serial processes occur during coal seam gas extraction: gas desorption from coal grains, gas diffusion through coal matrixes and then gas flow in cleat networks [6,7].

It should be noted that water and gas coexist in many coal seams, so two-phase flow is commonly present in cleats. To accurately describe gas transport process, the effective gas permeability expressed as a function of absolute permeability and relative gas permeability is often used [9-13]. However, the focus of this review work is on the absolute permeability of coal which, for simplification, is referred to as “permeability” throughout.

During primary CBM recovery, complex coal-gas interactions occur. When gas is extracted, the reduction of pore pressure leads to effective stress increase which results in fracture closure and permeability loss. As gas pressure declines below the desorption point, coal matrix starts to shrink because of methane desorption which in turn opens the fracture and increases permeability. The initial rapid loss in fracture

* Corresponding author.
E-mail addresses: qi.gao@research.uwa.edu.au, 935131241@qq.com, qi.gao@research.uwa.edu.au (Q. Gao).

https://doi.org/10.1016/j.fuel.2022.125124
Received 26 February 2022; Received in revised form 2 May 2022; Accepted 25 June 2022

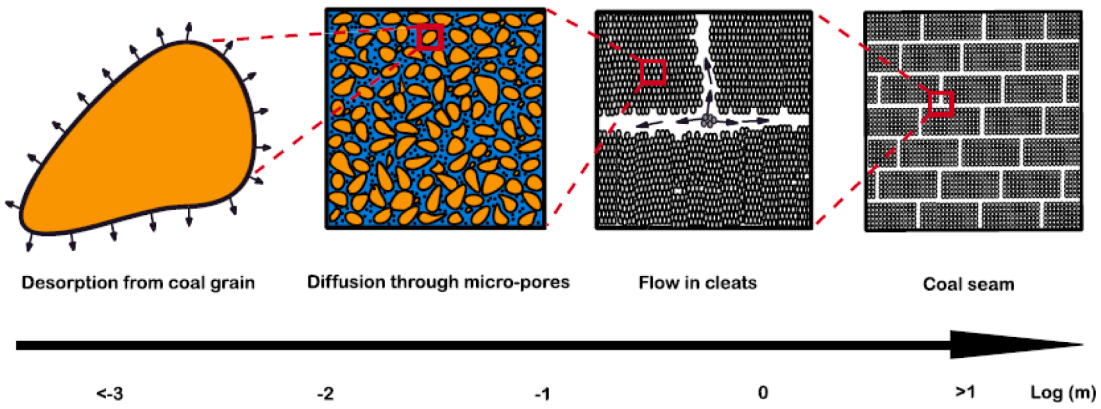

Fig. 1. Illustration of multiscale gas transport in coal seams [8].

permeability due to effective stress increase is supplemented by the later slow rebound in permeability due to matrix shrinkage. Whether the ultimate coal permeability is greater or less than the initial coal permeability depends on the net effect of the two opposing mechanisms [3,14-16]. Thus, a great challenge for simulating primary CBM recovery is the accurate prediction of coal permeability. Understanding coal permeability evolution behavior is also important for CO_2-ECBM recovery, which involves the injection of CO_2 to enhance CBM extraction [17-21]. Since coal has a greater sorption affinity for CO_2 than CH_4 at the same pressure [22], CO_2 injection not only enhances CBM production, but also provides a viable method to reduce greenhouse gas emissions. In addition, knowledge of change in permeability is necessary for evaluating coal mine safety [23-26]. With the increase of coal burial depth, gas content gradually increases. Coal and gas outburst may be triggered during mining operations as a result of gas accumulation. The accumulation of gas depends on many factors of which coal permeability is the most important one.

Great efforts have been made in the laboratory to investigate coal permeability evolution. Early laboratory experiments were conducted using water or air with the focus on permeability-stress relationship only [27-29]. More recently, experiments using various gases allow the measurement of the impact of stress as well as gas sorption-induced swelling on coal permeability change. Laboratory observation indicates that coal permeability values to strongly adsorbing gases like CO_2 and CH_4 are lower than those to lightly adsorbing or non-adsorbing gases like N_2 or He [30-32]. Commonly, laboratory experiments are conducted under two types of stress-controlled conditions: constant confining pressure (CCP) condition and constant effective stress (CES) condition. Under the CCP condition and for the gas injection tests, the evolution behavior of coal permeability can be classified into three categories: permeability increases with the increase of pore pressure [18,33-39]; permeability initially decreases and then rebounds with the increase of pore pressure [36,38,39]; permeability decreases with the increase of pore pressure [40,41]. Under the CCP condition and for the gas depletion tests, the evolution behavior of coal permeability can be classified into two categories: permeability decreases with the decrease of pore pressure [34,42,43]; permeability initially decreases and then rebounds with the decrease of pore pressure [34,35,43,44]. Under the CES condition and for the gas injection tests, all measured coal permeability data decrease with the increase of pore pressure [30,45-55]. Permeability of coal samples exposed to adsorbing gas is also found to be a function of gas sorption time [31,56-60].

Although laboratory experiments provide a cost-effective way to study permeability evolution, the measurements are conducted on small core samples, which may not represent the in-situ coal properties [61]. In addition, the applied stress-controlled conditions in the laboratory are different from the in-situ boundary conditions. Thus, the large-scale field tests can better uncover coal permeability evolution behavior under the reservoir condition. From the field tests, permeability of coal seams changes significantly during reservoir depletion, often exhibiting an increasing trend [11,62-70]. However, the opposite phenomenon has also been observed that permeability of coal seams decreases markedly during CO_2-ECBM recovery [71-77].

In summary, both field and laboratory tests indicate that the evolution of coal permeability is very complex during gas injection/extraction. In order to quantify and predict this change, a large variety of permeability models have been proposed in the last few decades. In this paper, the influencing factors of coal permeability are first summarized. Then, the classification criteria for coal permeability models are proposed. Based on these criteria, an in-depth review on the evolution of coal permeability models is conducted. In the following, a discussion on coal permeability models in each category is presented. Finally, the conclusions are made and the potential future research work for advancing our understanding on coal permeability is recommended.

2. Influencing factors of coal permeability

Coal permeability can be influenced by many factors [78,79]. The permeability models of coal are commonly defined as a function of these factors. Some models are based on only one factor while others consider multiple factors. Therefore, the applicability of these permeability models is different. In this section, the influencing factors of coal permeability are summarized.

2.1. Cleat parameters

It is widely accepted that the cleats in coal seams offer the main flow path for gas drainage [80-82]. Thus, coal permeability is predominantly attributed to the cleat networks while matrix blocks have a negligible contribution [83,84]. A range of cleat parameters may influence coal permeability value such as aperture, spacing, tortuosity, connectivity, orientation and mineral filling degree [78].

2.2. Stress

Coal seams are normally buried underground in depth of hundreds to thousands of meters [85], so coal bulk is tightly compressed by in-situ stresses. In addition, confining stress is commonly applied on core samples to measure coal permeability during laboratory experiments. Thus, coal permeability in both of the field and laboratory environments is closely related to the magnitude of applied stress. The increased stress tends to close the cleats and reduce the permeability of coal [29,32,86].

2.3. Gas sorption

A unique characteristic of coal is that the volume of coal changes

during gas sorption. Specifically, coal swells when gas adsorps while coal shrinks when gas desorps. Laboratory observations have revealed that gas sorption-induced coal volumetric strain can be up to a few percent [22,87-89]. This effect has an obvious impact on coal permeability under the reservoir condition since in-situ coal cleat porosity is significantly less than 1% [3,90].

2.4. Non-equilibrium state

In coal matrix, the micropore diameter is typically less than 50 nm; however, the fracture width is much larger and typically in the range of 3 to 10 μm [91]. Due to the significant permeability contrast between fracture and matrix, it may take several months or even a few years for gas injection/extraction induced local pressure difference to disappear. This spatially non-uniform pore pressure distribution and the associated non-uniform swelling strain in coal induces dynamic fracture-matrix interaction and leads to transient evolution of coal permeability [92,93].

2.5. Anisotropy and heterogeneity

As with other rocks, coal is naturally anisotropic. Field tests have shown that the anisotropy ratio of coal permeability can be as high as 17:1 [94]. Coal permeability anisotropy has also been confirmed in the laboratory experiments [95,96]. The main cause to coal permeability anisotropy is the existence of bedding planes [97] and directional cleat networks [98].

Coal heterogeneity can also result in permeability anisotropy. Many geological factors lead to coal heterogeneity including sediment sources, depositional environments, tectonic settings, diagenesis, climate and hydrological conditions [99]. In vertical direction, the composition of coal is strongly heterogeneous. Interbedded rocks are often found in coal seams [100]. In horizontal directions, coal is heterogeneous in terms of cleat density, internal cleat porosities and mineral matter distribution [42].

2.6. Creep

In general, coal is softer than other rocks, so the influence of creep on coal permeability is more pronounced. Creep in coal commonly occurs through four different mechanisms [101,102] including cataclastic creep, granular creep, pressure solution creep and adsorption-diffusion creep. During gas drainage, the latter two mechanisms may have more obvious impact on coal permeability than the other two mechanisms.

2.7. Damage

Coal damage may be induced by mining activities such as wellbore drilling, longwall mining, and roadway excavation [103,104]. The damage of coal and associated fracture propagation can lead to permeability enhancement up to thousands of times [103,105].

2.8. Temperature

The variation of temperature impacts coal permeability. Under high temperature, the rock thermoplastic strengthening makes the compression of coal easier [106] and the permeability is influenced as a result. In addition, temperature change influences gas adsorption performance in coal [107] and thus coal permeability is influenced. More importantly, temperature change induces thermal stress in coal [108] which can lead to coal deformation and permeability change.

2.9. Coal fines

Coal fines are often generated during CBM extraction as a result of the interaction between flowing fluid and coal solids affixed to cleat surface [9,109,110]. Some of these coal fines may settle down within the cleat networks during the migration process, which can narrow or even plug the cleats. Thus, generation of coal fines may lead to coal permeability reduction.

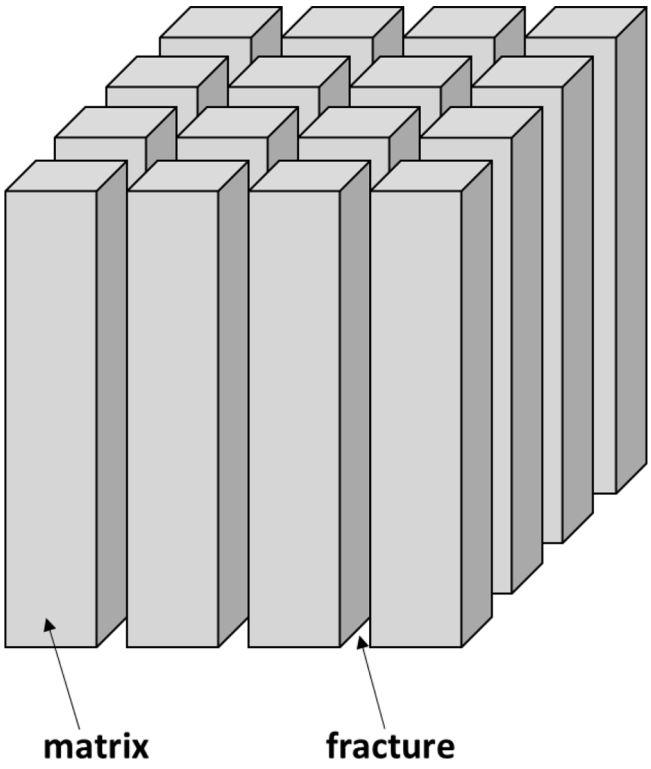

Fig. 2. Idealization of coal as the matchstick geometry with through-going fractures.

3. Evolution of coal permeability models

Most coal permeability models have taken the combined effects of stress and gas sorption into account, but they may have a variety of forms when specific coal structure and boundary conditions are imposed. To describe the internal structure of coal, matchstick geometry, cubic geometry and the geometry containing rock bridges are commonly used to represent the fracture-matrix system. In matchstick and cubic geometries, matrix blocks are completely separated from each other by through-going fractures while in the geometry containing rock bridges adjacent matrix blocks are connected with each other. Only the geometry containing rock bridges takes into account gas sorption-induced fracture-matrix interaction and considers the difference between coal bulk sorption strain, matrix sorption strain and fracture sorption strain. To describe the stress state in coal, a range of boundary conditions from stress-controlled to displacement-controlled are used. For the field tests, either the uniaxial strain or the constant volume condition is commonly assumed while for laboratory experiments CCP and CES conditions are commonly used. Additionally, in recent years, both laboratory experiments and theoretical analysis have indicated that the local non-equilibrium between fracture and matrix systems has a significant impact on coal permeability evolution.

In this paper, coal permeability models are classified according to internal structure of coal, boundary conditions and equilibrium state within the controlled volume. Based on these classification criteria, coal permeability models can be classified into two major categories. One category is structure-based equilibrium models including matchstick models, cubic models and rock bridge models. The other category is structure-based non-equilibrium models. In each category, we review the format, theoretical assumptions, influencing factors and applications of these permeability models.

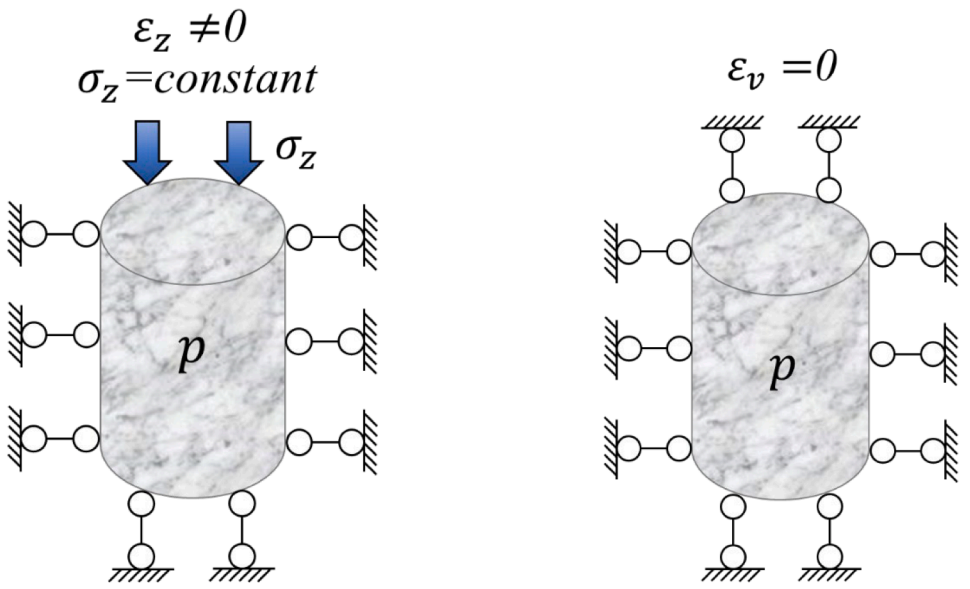

(a) Uniaxial strain & constant vertical stress condition (b) Constant volume condition

Fig. 3. Schematic diagram of the in-situ boundary conditions.

3.1. Category 1 – Structure-based equilibrium models

3.1.1. Matchstick models

In the initial stage, permeability models are derived for analyzing gas flow in coal seams under the in-situ conditions. As shown in Fig. 2, matchstick geometry is typically assumed for coal seams. This is because most coal seams being developed are nearly horizontal and contains nearly vertical cleat networks and horizontal bedding planes. However, the horizontal bedding planes are probably closed and contribute little to gas flow due to the relatively large overburden stress [29,111].

For the producing coal seams, most work assumes that the uniaxial strain and constant vertical stress condition should be applied. Under this condition, the vertical stress remains unchanged, no displacement is allowed in the horizontal direction and coalbeds can only move along the vertical direction. In addition, the concept of coal seams under the constant volume condition is also proposed [111-113] although it is difficult to justify it. Fig. 3 shows the bounding behavior of the two different boundary conditions.

By imposing the matchstick geometry, in-situ boundary conditions and equilibrium state, various models for analyzing permeability response of coal seams are developed. It should be noted that coal geometry is not specified in some models but these models are still included because of the suited boundary conditions.

Equations for porosity and permeability of collections of slabs, matchsticks and cubes were first derived by Reiss [114]. Idealizing coalbed as a collection of matchsticks and assuming fluid flow along the axial direction of these matchsticks, Seidle et al. [29] defines coal permeability as a function of hydrostatic stress. McKee et al. [115] designed a stress-dependent coal permeability model as well and these two models have the similar form.

Considering coal permeability to be primarily controlled by the horizontal stresses acting on the cleat surfaces, Gray [14], Gilman and Beckie [116], and Shi and Durucan [3] derived the expressions for effective horizontal stress in the state of uniaxial strain. Equating the effective horizontal stress under the uniaxial strain condition with the hydrostatic stress in the model by Seidle et al. [29] gives permeability model for in-situ coal seams. Note that gas sorption contributes to horizontal stress variation in these models. Among them, Gray [14] was the first to incorporate both the influence of reservoir stress and matrix shrinkage into coal permeability model. Different from the assumption that it is the horizontal stresses normal to cleat surfaces dominating coal permeability change, Cui and Bustin [117] related coal permeability with mean normal stress. As these four models have the similar form, only the model proposed by Cui and Bustin [117] is presented here:

$$\frac{k}{k_0} = exp\left\{\frac{3}{K_p}\left[\frac{1+v}{3(1-v)}(p-p_0) - \frac{2E}{9(1-v)}(\varepsilon_s - \varepsilon_{s0})\right]\right\} \quad (1)$$

where the subscript "0" denotes the initial state, k is coal permeability, p is pore pressure, K_p is fracture modulus, v is Poisson's ratio, E is elastic modulus, and ε_s is gas sorption strain.

Assuming that coal permeability change is due to pore compressibility and gas sorption, Sawyer et al. [120,121] developed the ARI model. In this model, matrix swelling is assumed to be proportional to the adsorbed gas concentration. Pekot and Reeves [122,123] extended the ARI model by considering the effect of differential swelling.

Palmer and Mansoori [124] proposed another widely used coal permeability model considering that pore pressure variation and gas desorption-induced matrix shrinkage are the main causes for permeability change. Because original P&M model [124] fails to match the reservoir data from San Juan basin, an improvement was made by Palmer et al. [86] for better matching the observed permeability variation. In the modified model, cleat anisotropy and pressure-dependent bulk modulus were considered.

Assuming constant vertical stress, Levine [118] derived a model for coal fracture width which is equal to the sum of three terms: the initial fracture width, closure due to fracture compressibility and opening due to matrix shrinkage:

Some other studies ignore the impact of stress on coal permeability and consider the role of gas sorption alone such as Seidle and Huitt [119] and Harpalani and Chen [45,111].

Anisotropy is another important factor that will significantly impact coal permeability. Assuming matchstick coal geometry, Gu and Chalaturnyk [125] developed a permeability model which incorporates the joint impacts of coalbed anisotropy, in-situ stress, gas sorption, and temperature change. This work is extended by Gu and Chalaturnyk [126] through treating the discontinuous coal mass as an equivalent elastic continuum. To evaluate coal permeability change caused by

Table 1
Summary of coal permeability models under matchstick geometry & in-situ boundary conditions & equilibrium state.

Model Sources	Format	Theoretical assumptions	Influencing factors	Applications
Gray [14]	$k = f(p)$	Uniaxial strain and constant vertical stress condition & Local equilibrium	Stress & Gas sorption	Field data analysis
Sawyer et al. [120,121]	$k = f(p)$	Constant vertical stress condition & Local equilibrium	Pore pressure & Gas sorption	Field data analysis
Seidle et al. [29]	$k = f(p)$	Matchstick geometry & Uniaxial strain and constant vertical stress condition & Local equilibrium	Stress	Field data analysis
Seidle and Huitt [119]	$k = f(p)$	Matchstick geometry & Uniaxial strain condition & Local equilibrium	Gas sorption	Field data analysis
Harpalani and Chen [45,111]	$k = f(p)$	Matchstick geometry & Constant volume condition & Local equilibrium	Gas sorption	Field data analysis
Levine [118]	$k = f(p)$	Slab geometry & Constant vertical stress condition & Local equilibrium	Stress & Gas sorption	Field data analysis
Palmer and Mansoori [124]	$k = f(p)$	Matchstick geometry & Uniaxial strain and constant vertical stress condition & Local equilibrium	Pore pressure & Gas sorption	Field data analysis
Gilman and Beckie [116]	$k = f(p)$	Uniaxial strain and constant vertical stress condition & Local equilibrium	Stress & Gas sorption	Field data analysis
Pekot and Reeves [122,123]	$k = f(p)$	Constant vertical stress condition & Local equilibrium	Pore pressure & Gas sorption	Field data analysis
Shi and Durucan [3]	$k = f(p)$	Matchstick geometry & Uniaxial strain and constant vertical stress condition & Local equilibrium	Stress & Gas sorption	Field data analysis
Cui and Bustin [117]	$k = f(p)$	Matchstick geometry & Uniaxial strain and constant vertical stress condition & Local equilibrium	Stress & Gas sorption	Field data analysis
*Gu and Chalaturnyk [125,126]	$k = f(\epsilon)$	Matchstick geometry & Uniaxial strain condition & Local equilibrium	Stress & Gas sorption & Temperature & Anisotropy	Field data analysis
Pan and Connell [127]	$k = f(p)$	Uniaxial strain and constant vertical stress condition & Local equilibrium	Stress & Gas sorption & Anisotropy	Field data analysis
Ma et al. [112]	$k = f(p)$	Matchstick geometry & Constant volume condition & Local equilibrium	Stress & Gas sorption	Field data analysis

"p" represents pore pressure.
"ϵ" represents strain.
* The permeability models proposed by Gu and Chalaturnyk [125,126] are expressed as a function of strain instead of pore pressure. This is because the expressions haven't been reduced to the simplest form.

anisotropic swelling, Pan and Connell [127] developed a model considering the anisotropic coal matrix swelling and thermal expansion. Their start point was the constitutive relationship for anisotropic poroelastic medium with orthorhombic symmetry [128].

Massarotto et al. [113] suggested that coalbeds are actually under a constant volume condition. Ma et al. [112] and Harpalani and Chen [45,111] designed coal permeability models on the basis of constant volume theory in which the decrease in the dimension of coal matrix should be equal to the increase in the dimension of cleat aperture. The models mainly focus on the changes of matrix and cleat volumes and are, therefore, different from other models that lay heavy emphasis on matrix and cleat compressibility.

To figure out the common features of matchstick models, the model format, assumptions, influencing factors and applications are summarized, as shown in Table 1. In most of these models, three assumptions are made: (1) matchstick geometry is assumed for the internal structure of coal; (2) in-situ boundary conditions are assumed either as the uniaxial strain condition or the constant volume condition; and (3) equilibrium state is achieved between fracture and matrix within the representative elementary volume (REV). For influencing factors, stress and gas sorption play the controlling role for coal permeability change. In terms of applications, permeability models are specifically designed for analyzing field data and simulating reservoir gas flow. As for the model format, coal permeability is defined as a function of pore pressure.

3.1.2. Cubic models

Matchstick models are derived under in-situ boundary conditions either as the uniaxial strain or constant volume condition. For uniaxial strain condition, coal deformation in horizontal plane is zero but in vertical direction it may occur. For constant volume condition, coal deformation is restricted in all directions. However, in the laboratory, coal permeability is commonly measured under stress-controlled conditions where the external surface of coal is free to deform. Therefore, application of matchstick models to predict coal permeability change under laboratory-used stress-controlled conditions will

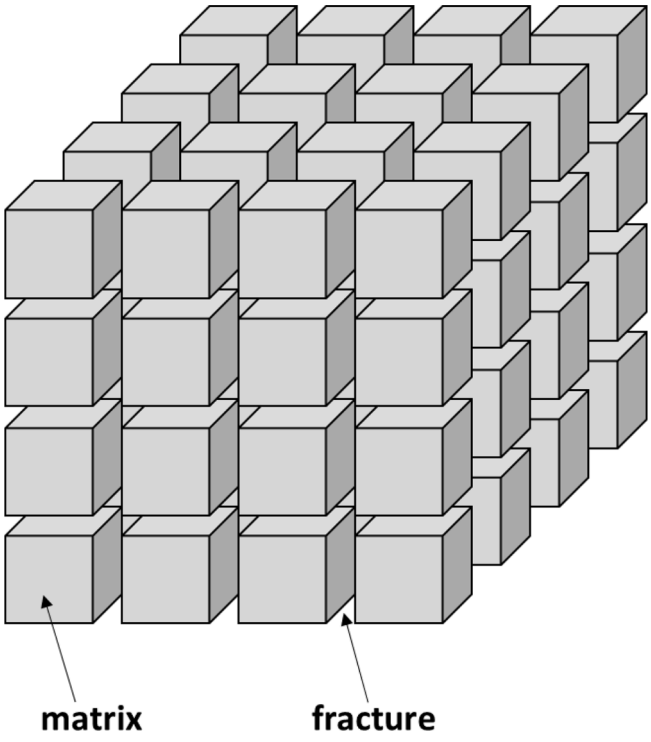

Fig. 4. Idealization of coal as the cubic geometry with through-going fractures.

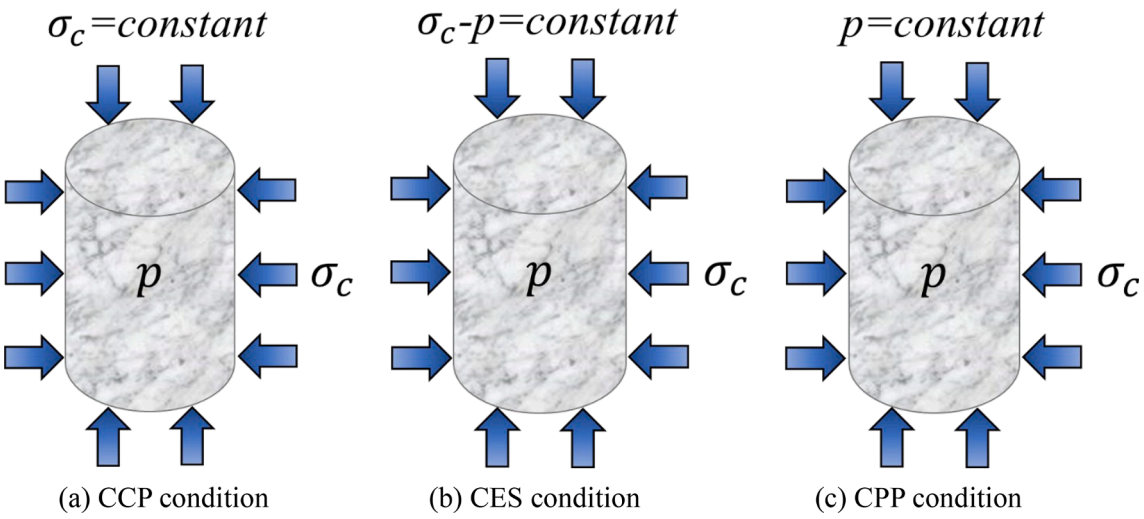

Fig. 5. Schematic diagram of the laboratory-used boundary conditions.

exaggerate the effect of gas sorption-induced strain [38]. To provide a more reasonable predicting result, models for laboratory use must be derived.

To this end, cubic geometry is typically assumed, as shown in Fig. 4. Cleats are found to be oriented orthogonally in coal samples in the laboratory [129] as confining stress is applied uniformly to the outer surface of coal samples during the experiments. This implies that three sets of orthogonal fractures contribute to the gas flow.

In laboratory experiments, two different boundary conditions are commonly used, i.e., CCP condition and CES condition. Sometimes, constant pore pressure (CPP) condition is also used. Fig. 5 shows the bounding behavior of the three boundary conditions. For CCP condition, confining pressure is kept unchanged throughout the experiments. For CES condition, the difference between confining pressure and pore pressure is kept unchanged throughout the experiments. For CPP condition, injection pressure is kept unchanged throughout the experiments.

By imposing cubic geometry, variable stress conditions and equilibrium state, models for analyzing coal permeability response in the laboratory environment are developed. It should be noted that coal geometry is not specified in some models but these models are still included because of the suited boundary conditions.

Robertson and Christiansen [129,130] designed an analytical model for predicting permeability change caused by gas sorption in the fractured coal under two typical laboratory conditions including CCP condition and CPP condition. The model approximated coal matrix blocks as the cubic geometry. In their derivation, permeability change is related to three different factors including fracture compressibility, matrix modulus and sorption-induced strain.

Applying the poroelastic theory, Zhang et al. [131] and Liu et al. [96,132] proposed a general coal porosity and permeability model which can be used to explain permeability responses from stress-controlled to displacement-controlled conditions. Based on these works, Cao et al. [133] obtained the relationship between coal permeability and effective stress/strain under variable stress conditions in another form:

$$\frac{k}{k_0} = exp\left\{ -\frac{3}{K_p}[(\overline{\sigma} - \overline{\sigma}_0) - (p - p_0)] \right\} \tag{2}$$

$$\overline{\sigma} - p = -K\left(\varepsilon_v + \frac{p}{K_s} - \varepsilon_s\right) \tag{3}$$

where $\overline{\sigma}$ denotes mean normal stress, K is coal bulk modulus, ε_v is volumetric strain of coal, and K_s is coal matrix modulus.

Table 2
Summary of coal permeability models under cubic geometry & variable stress conditions & equilibrium state.

Model Sources	Format	Theoretical assumptions	Influencing factors	Applications
Robertson and Christiansen [129,130]	$k = f(\sigma,p)$	Cubic geometry & Variable stress conditions & Local equilibrium	Stress & Gas sorption	Lab data analysis
Zhang et al. [131]	$k = f(\varepsilon_e)$	Variable stress conditions & Local equilibrium	Stress & Gas sorption	Lab & Field data analysis
Liu et al. [96,132]	$k = f(\varepsilon_e)$	Variable stress conditions & Local equilibrium	Stress & Gas sorption & Temperature	Lab & Field data analysis
Cao et al. [133]	$k = f(\varepsilon_e)$	Variable stress conditions & Local equilibrium	Stress & Gas sorption	Lab & Field data analysis
Wu et al. [81]	$k = f(\sigma,p)$	Cubic geometry & Variable stress conditions & Local equilibrium	Stress & Gas sorption	Lab data analysis
Wu et al. [82]	$k = f(\sigma,p)$	Cubic geometry & Variable stress conditions & Local equilibrium	Stress & Gas sorption & Anisotropy	Lab data analysis
Wang et al. [134]	$k = f(\sigma,p)$	Cubic geometry & Variable stress conditions & Local equilibrium	Stress & Gas sorption & Anisotropy	Lab data analysis

"σ" represents total stress, and "p" represents pore pressure.
"ε_e" represents effective strain.

Wu et al. [81,82] established a dual porosity model for coal seams under variable stress conditions and then extended their model to define the evolution of gas sorption-induced permeability anisotropy. Wang et al. [134] developed a model by integrating the mechanical and textural properties to describe coal permeability anisotropy. With directional strains, the permeability of coal in any direction can be calculated.

To figure out the common features of cubic models, the model

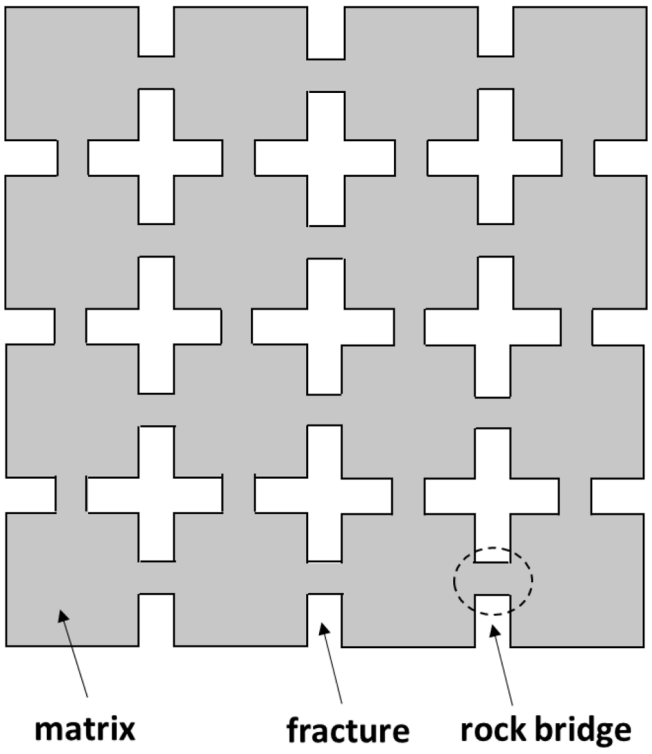

Fig. 6. Schematic diagram of coal structure containing rock bridges.

format, assumptions, influencing factors and applications are summarized, as shown in Table 2. In most of these models, three assumptions are made: (1) cubic geometry is assumed for the internal structure of coal; (2) coal is under variable stress conditions; and (3) the equilibrium state is achieved between fracture and matrix within REV. For the influencing factors, stress and gas sorption play the controlling role for coal permeability change. In terms of applications, permeability models can be used to analyze laboratory data. As for the model format, coal permeability is defined as a function of effective stress/strain. It should be mentioned that some models in this table do not consider the geometry of coal. These models ignoring coal geometry can be applied to analyze both laboratory and field data.

3.1.3. Rock bridge models

When experimental data are interpreted, coal geometry with matrix blocks completely separated from each other is commonly assumed. In this arrangement, for a given injection pressure, gas sorption-induced matrix swelling/shrinkage will not contribute to the coal permeability change under the laboratory-used CCP condition [135,136]. When an adsorptive gas such as CO_2 is injected into coal, pressure in the fracture will reach the injection pressure instantly. At this moment, the maximum pressure difference is created between the fracture and matrix. As gas diffuses into the matrix, the pressure difference gradually diminishes. In this stage, matrix swells as a result of gas adsorption and effective stress decline in it. Because the effective stress in fracture remains constant in the whole process, coal matrix swelling only increases fracture spacing rather than changes the fracture aperture. In other words, 0% of the swelling/shrinkage strain contributes to the permeability change of fractured coal under the CCP condition. However, this is not consistent with many laboratory observations that matrix swelling shows significant impact on coal permeability [18,45,47].

Liu and Rutqvist [136] believed that the above discrepancy is due to the oversimplification of coal structure and thus they proposed a new coal structure in which adjacent matrix blocks are not completely separated from each other but connected through the rock bridges, as shown in Fig. 6. In their work, a new concept called "internal swelling stress" was introduced to account for gas sorption-induced fracture-matrix interaction on coal permeability change. Based on this new concept, coal matrix swelling strain was divided into two components: one for the bulk strain and the other for the fracture strain. Considering the impact of fracture-matrix interaction, coal permeability models

Table 3
Summary of coal permeability models under the geometry containing rock bridges & variable stress conditions & equilibrium state.

Model Sources	Format	Theoretical assumptions	Influencing factors	Applications
Liu and Rutqvist [136]	$k = f(p)$	Rock bridges & Variable stress conditions & Local equilibrium	Stress & Gas sorption	Lab & Field data analysis
Connell et al. [135]	$k = f(\sigma,p,f)$	Rock bridges & Variable stress conditions & Local equilibrium	Stress & Gas sorption	Lab data analysis
Chen et al. [137]	$k = f(\sigma,p,f)$	Rock bridges & Variable stress conditions & Local equilibrium	Stress & Gas sorption	Lab data analysis
Guo et al. [138]	$k = f(\sigma,p,f)$	Rock bridges & Variable stress conditions & Local equilibrium	Stress & Gas sorption	Lab data analysis
Wang et al. [139]	$k = f(\sigma,p,f)$	Rock bridges & Variable stress conditions & Local equilibrium	Stress & Gas sorption & Anisotropy	Lab data analysis
Lu et al. [140]	$k = f(\sigma,p,f)$	Rock bridges & Variable stress conditions & Local equilibrium	Stress & Gas sorption	Lab & Field data analysis
Liu et al. [141]	$k = f(\sigma,p,f)$	Rock bridges & Variable stress conditions & Local equilibrium	Stress & Gas sorption	Lab & Field data analysis
Yang et al. [142]	$k = f(\varepsilon_e,f)$	Variable stress conditions & Local equilibrium	Stress & Gas sorption	Lab & Field data analysis
Wang et al. [59]	$k = f(\sigma,p,f)$	Rock bridges & Variable stress conditions & Local equilibrium	Stress & Gas sorption	Lab data analysis
Zhou et al. [143]	$k = f(\varepsilon_e,f)$	Rock bridges & Variable stress conditions & Local equilibrium	Stress & Gas sorption & Creep	Lab data analysis
Shi et al. [144]	$k = f(\sigma,p,f)$	Rock bridges & Variable stress conditions & Local equilibrium	Stress & Gas sorption	Lab data analysis
Li et al. [145]	$k = f(\varepsilon_e,f,R_m)$	Rock bridges & Variable stress conditions & Local equilibrium	Stress & Gas sorption & Anisotropy	Lab & Field data analysis
Peng et al. [146]	$k = f(\sigma,p,f)$	Rock bridges & Variable stress conditions & Local equilibrium	Stress & Gas sorption	Lab data analysis
Jiang et al. [147]	$k = f(\sigma,p,f)$	Rock bridges & Variable stress conditions & Local equilibrium	Stress & Gas sorption	Lab & Field data analysis
Liu et al. [148]	$k = f(\varepsilon_e,R_m)$	Rock bridges & Variable stress conditions & Local equilibrium	Stress & Gas sorption	Lab & Field data analysis

"σ" represents total stress, and "p" represents pore pressure.
"ε_e" represents effective strain.
"f" represents strain splitting factor or strain splitting function.

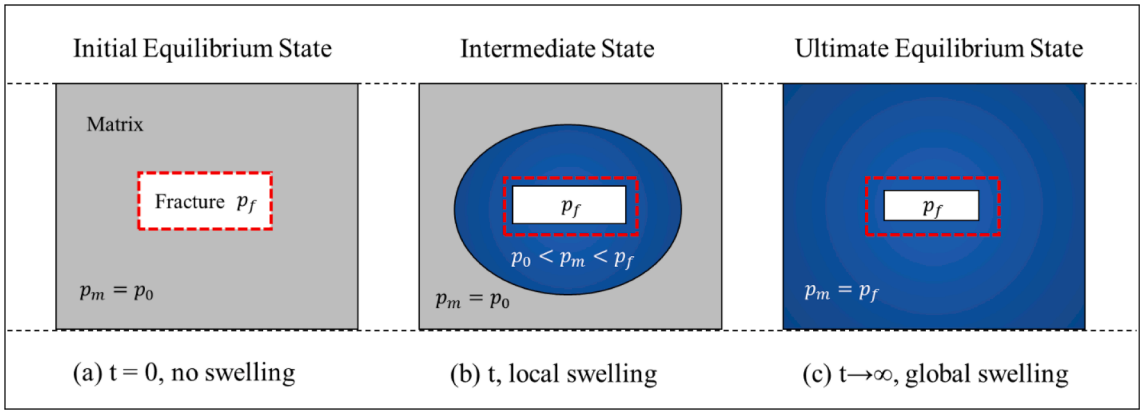

Fig. 7. Transient evolution of gas pressure and fracture aperture within REV under the constant volume condition.

under the uniaxial strain condition and CCP condition are developed.

Many other scholars also find that the role of rock bridge on coal permeability change should not be ignored. When matrix swells, fracture is compressed as fracture itself is weak and soft structure in coal. Meanwhile, rock bridge prevents matrix swelling from completely closing the fracture. Therefore, part of matrix swelling strain contributes to fracture deformation and the remaining results in coal bulk deformation. To distinguish sorption-induced coal bulk strain, matrix strain and fracture strain, Connell et al. [135], Chen et al. [137], Guo et al. [138], Wang et al. [139], Lu et al. [140], Liu et al. [141], Yang et al. [142], Wang et al. [59], Zhou et al. [143], Shi et al. [144], and Li et al. [145] defined the strain splitting factor and incorporated it into the permeability model to account for fracture-matrix interaction. As these models have the similar form, only the model proposed by Connell et al. [135] is presented here. Connell et al. [135] derived permeability model in two general forms. One is exponential form and the other is cubic form. For the exponential form, assuming constant cleat compressibility, coal permeability ratio was approximated as:

$$\frac{k}{k_0} = exp\left\{-3\left[c_{pc}^{(M)}\left(\widetilde{\sigma}_c - \widetilde{p}_p\right) - (1-\varphi)\widetilde{\varepsilon}_b^{(s)}\right]\right\} \tag{4}$$

For the cubic form, coal permeability ratio was given by:

$$\frac{k}{k_0} = \left\{1 - \frac{1}{\varnothing_0}\left[\frac{1}{K}\left(\widetilde{\sigma}_c - \widetilde{p}_p\right) - (\beta-1)\widetilde{\varepsilon}_b^{(s)}\right]\right\}^3 \tag{5}$$

where $c_{pc}^{(M)}$ is cleat compressibility, $\widetilde{\sigma}_c$ is increments of confining stress, $\widetilde{p}_p$ is increments of pore pressure, $\widetilde{\varepsilon}_b^{(s)}$ is increments of bulk sorption strain, and φ and β are two different strain splitting factors which relate pore sorption strain and matrix sorption strain to the bulk sorption strain:

$$\widetilde{\varepsilon}_p^{(s)} = \varphi\widetilde{\varepsilon}_b^{(s)} \tag{6}$$

$$\widetilde{\varepsilon}_m^{(s)} = \beta\widetilde{\varepsilon}_b^{(s)} \tag{7}$$

where $\widetilde{\varepsilon}_p^{(s)}$ is pore sorption strain, and $\widetilde{\varepsilon}_m^{(s)}$ is matrix sorption strain.

The above permeability models use a constant strain splitting factor to distinguish different gas sorption strains. Unlike these models, Peng et al. [146] and Jiang et al. [147] introduced the strain splitting function to define the relation among gas sorption-induced strains in coal.

Liu et al. [148] pointed out that the rock bridges between adjacent matrix blocks play an important role in fracture-matrix interaction. They accommodated sorption-induced swelling strains both over the rock bridges that hold fractures open but also over the intervening free faces that compress the fractures. Under this condition, coal permeability model was built through treating the fractured coal mass as an equivalent continuous medium and introducing the modulus reduction ratio R_m.

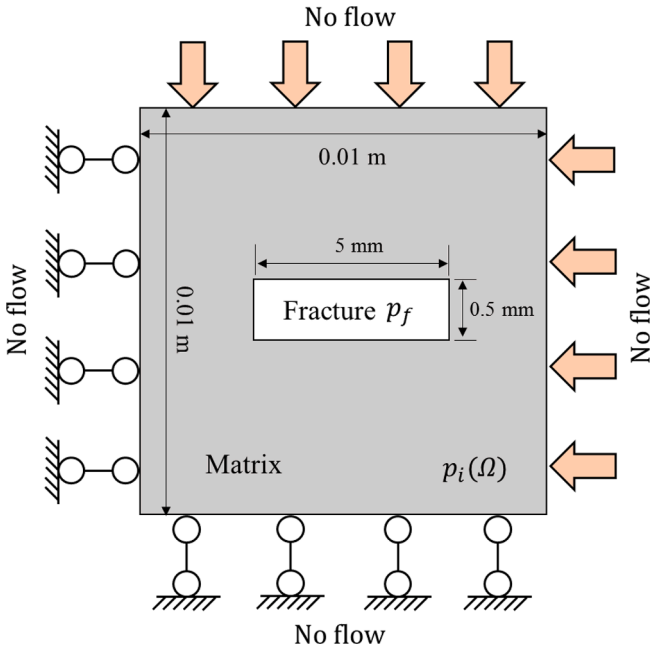

Fig. 8. Single fracture non-equilibrium model to represent the permeability response of coal under unconstrained swelling condition.

To figure out the common features of rock bridge models, the model format, assumptions, influencing factors and applications are summarized, as shown in Table 3. In most of these models, three assumptions are made: (1) rock bridges are contained in the internal structure of coal; (2) coal is under variable stress conditions; and (3) equilibrium state is achieved between fracture and matrix within REV. For influencing factors, stress and gas sorption play the controlling role for coal permeability change. In terms of applications, permeability models can be used to analyze both laboratory and field data. As for the model format, coal permeability is defined as a function of effective stress/strain and the strain splitting factor/function.

3.2. *Category 2 – Structure-based non-equilibrium models*

For matchstick, cubic and rock bridge models, the assumption of local equilibrium between fracture and matrix within REV is made. Due to this assumption, gas pressure and the associated swelling strain within REV is always uniform. This uniform state only represents the ultimate equilibrium between fracture and matrix. However, for unconventional gas reservoirs such as coal seams, the matrix permeability

is normally several orders of magnitude lower than the fracture permeability. Because of the naturally huge contrast between fracture and matrix properties, local non-equilibrium lasts for a very long time within REV due to the kinetic diffusion of gas through coal matrix [117]. Thus, the evolution process of coal permeability from initial equilibrium to ultimate equilibrium may be much more important than that value at ultimate equilibrium. In order to clearly illustrate this evolution process, Fig. 7 presents the gas pressure dissipation in coal matrix and the dynamic variation of fracture aperture induced by gas sorption under the constant volume condition.

3.2.1. Single fracture non-equilibrium models

Liu et al. [92] first performed the explicit simulations of dynamic interaction between coal matrix and fracture. In their study, a fully coupled numerical approach was applied to recover important nonlinear responses of coal permeability due to the gas adsorption and effective stress effect under stress-controlled conditions. Fig. 8 presents the geometry, initial and boundary conditions of the numerical model. The size of the model is 1.0 cm by 1.0 cm with a rectangular fracture in the center. The fracture length and width are 5 mm and 0.5 mm, respectively. Roller boundary condition was applied on the left and bottom sides of the model, and the right and upper sides were stress-controlled. No flow boundary condition was set for all the outer sides and injection pressure was exerted on the fracture surfaces. The coupled equations governing coal matrix deformation, gas transport, and porosity and permeability variation were defined. A detailed introduction of these equations will not be provided here. The results of this work indicated that the transition of coal matrix swelling from local swelling to global swelling is the fundamental mechanism for the switching of permeability from reduction to enhancement.

Applying the same method as above, Chen et al. [149] explicitly modeled the dynamic fracture-matrix interaction incorporating the heterogeneous distribution of Young's modulus and Langmuir strain constant in the vicinity of the fracture. Qu et al. [150,151] developed the fully coupled coal deformation, gas flow, and thermal transport models. These combined effects were evaluated through explicit simulation of the dynamic fracture-matrix interaction. Liu et al. [152] proposed a numerical model to study the time-dependent coal permeability evolution behavior. The permeability variation was tracked until the final equilibrium state was reached. In their model, coal fracture was treated as a type of soft inclusion instead of a void. Wei et al. [153] numerically simulated the dynamic fracture-matrix interaction with the assumption that Young's modulus of the fracture is much lower than that of the surrounding matrix. In their model, the field equations governing solid deformation and gas transport for both the fracture and matrix were defined.

For better describing coal permeability evolution behavior, three common assumptions including uniaxial strain, constant overburden stress and local equilibrium were relaxed by Peng et al. [154] through considering the effective stress transfer between fracture and matrix. Assuming a fracture in the center of a cylinder, a fully coupled numerical approach was applied to generate the permeability profiles against time under various boundary conditions.

Moreover, analytical methods can also be used to capture the transient evolution behavior of coal permeability. Zeng et al. [155-157] introduced a novel concept called "volumetric ratio" to quantify the impact of matrix swelling area propagation on coal permeability change. The volumetric ratio was defined as the ratio of gas invaded area to the whole matrix area. Liu et al. [158] also studied the impact of non-uniform swelling on coal permeability evolution from initial to ultimate equilibrium state. In their work, the fracture aperture change was represented through an averaging method after obtaining the matrix swelling distribution within REV.

3.2.2. Upscaling non-equilibrium models

Although coal permeability transient behavior is well captured by single fracture non-equilibrium models, the geomechanical responses of coal at the reservoir scale during gas injection/extraction cannot be simulated, which limits the application of these models.

In order to solve the problem, Peng et al. [159] first proposed an upscaling non-equilibrium model. The model was established through defining four different strains including coal global strain, fracture local strain, matrix global strain, and pore local strain. Both the porosity and permeability of fracture and matrix in coal were expressed as a function of these strains. With the purpose of upscaling the permeability model to reservoir scale, Peng et al. [159] applied the overlapping continua

Table 4
Summary of coal permeability models under the geometry containing rock bridges & variable stress conditions & non-equilibrium state.

Model Sources	Format	Theoretical assumptions	Influencing factors	Applications
Liu et al. [92]	$k = f(\varepsilon_e, t)$	Rock bridges & Variable stress conditions	Stress & Gas sorption & Local non-equilibrium	Lab and field data analysis
Chen et al. [149]	$k = f(\varepsilon_e, t)$	Rock bridges & Variable stress conditions	Stress & Gas sorption & Local non-equilibrium & Heterogeneity	Lab and field data analysis
Qu et al. [150]	$k = f(\varepsilon_e, t)$	Rock bridges & Variable stress conditions	Stress & Gas sorption & Local non-equilibrium & Temperature	Lab and field data analysis
Qu et al. [151]	$k = f(\varepsilon_e, t)$	Rock bridges & Variable stress conditions	Stress & Gas sorption & Local non-equilibrium & Temperature	Lab and field data analysis
Liu et al. [152]	$k = f(\varepsilon_e, t)$	Rock bridges & Variable stress conditions	Stress & Gas sorption & Local non-equilibrium	Lab and field data analysis
Wei et al. [153]	$k = f(\varepsilon_e, t)$	Rock bridges & Variable stress conditions	Stress & Gas sorption & Local non-equilibrium	Lab and field data analysis
Peng et al. [154]	$k = f(\varepsilon_e, t)$	Rock bridges & Variable stress conditions	Stress & Gas sorption & Local non-equilibrium	Lab and field data analysis
Zeng et al. [155]	$k = f(\sigma, p, t)$	Rock bridges & Variable stress conditions	Stress & Gas sorption & Local non-equilibrium	Lab data analysis
Zeng et al. [156]	$k = f(\sigma, p, t)$	Rock bridges & Variable stress conditions	Stress & Gas sorption & Local non-equilibrium & Heterogeneity & Pore types	Lab data analysis
Zeng et al. [157]	$k = f(\sigma, p, t)$	Rock bridges & Variable stress conditions	Stress & Gas sorption & Local non-equilibrium	Lab data analysis
Liu et al. [158]	$k = f(\varepsilon_e, t)$	Rock bridges & Variable stress conditions	Stress & Gas sorption & Local non-equilibrium	Lab data analysis
Peng et al. [159]	$k = f(\varepsilon_e, t)$	Rock bridges & Variable stress conditions	Stress & Gas sorption & Local non-equilibrium	Lab and field data analysis
Zhu et al. [160]	$k = f(\varepsilon_e, t)$	Rock bridges & Variable stress conditions	Stress & Gas sorption & Local non-equilibrium & Damage	Lab and field data analysis
Zhang et al. [161]	$k = f(\varepsilon_e, t)$	Rock bridges & Variable stress conditions	Stress & Gas sorption & Local non-equilibrium	Lab and field data analysis
Wei et al. [162]	$k = f(\varepsilon_e, t)$	Rock bridges & Variable stress conditions	Stress & Gas sorption & Local non-equilibrium	Lab and field data analysis
Huang et al. [163]	$k = f(\varepsilon_e, t)$	Rock bridges & Variable stress conditions	Stress & Gas sorption & Local non-equilibrium	Lab and field data analysis

"σ" represents total stress, and "p" represents pore pressure.
"ε_e" represents effective strain.
"t" represents time.

approach to describe the dynamic interaction between fracture and matrix. In this approach, coal was represented as three overlapping and interacting physical fields: (1) coal deformation field; (2) gas flow field in the fracture; and (3) gas diffusion field in the matrix. On the basis of this work, Zhu et al. [160] extended the upscaling dual porosity model by considering the coal damage induced by gas adsorption. Applying the same approach, an improved upscaling non-equilibrium model was built by Zhang et al. [161] to explore the mechanisms behind coal permeability change as well.

To investigate the impact of non-equilibrium state on coal permeability evolution, Wei et al. [162] extended the conventional dual porosity model to include the equilibrium time lag between matrix and fracture. In this work, the matrix REV was divided into two sub-REVs by using the well-known multiple interacting continua (MINC) approach. The time lag effect was defined as a function of the strain difference between matrix REV and sub-matrix REV. Then, the strain function was incorporated into the coal permeability model.

As conventional dual porosity/permeability models cannot capture the true transient nature of fracture-matrix interactions in coal, Huang et al. [163] developed a transient dual porosity/permeability model which can capture the real gas diffusion process in coal matrix. This is achieved through embedding of a local REV structure into the overall multiphysics framework. The inclusion of transient process in matrix system enables the accurate modelling of coal permeability whole evolution process from initial to ultimate equilibrium.

To figure out the common features of non-equilibrium models, the model format, assumptions, influencing factors and applications are summarized, as shown in Table 4. In these models, two assumptions are made: (1) rock bridges are contained in the internal structure of coal; and (2) coal is under variable stress conditions. For influencing factors, stress, gas sorption and local non-equilibrium between fracture and matrix jointly play the controlling role for coal permeability change. In terms of applications, permeability models can be used to analyze both laboratory and field data. As for the model format, coal permeability is defined as a function of effective stress/strain and the gas sorption time.

4. Discussion on coal permeability models in each category

Matchstick models are derived under in-situ boundary conditions either as the uniaxial strain or the constant volume condition. Among these models, P&M model [124] is often used to match the in-situ coal permeability but it fails to match the reservoir data from San Juan basin. After improvement, the revised form of P&M model can match two groups of San Juan basin permeability data only under three rigorous preconditions [164]. S&D model [3] is another representative work. Permeability values predicted by this model have a good agreement with the reservoir permeability data from two different sites of San Juan basin. However, comparison of the widely used P&M model and S&D model with laboratory-measured coal permeability data shows that these two models fail to match the experimental observation and obviously exaggerate the effect of gas sorption-induced strain on coal permeability change [38]. The main reason for the failure is that both P&M model and S&D model were derived to represent in-situ reservoir conditions while laboratory coal permeability data are typically measured under variable stress conditions in which the confining pressure is applied uniformly to the external surface of the tested sample [129]. The laboratory-used boundary conditions are obviously different from the in-situ boundary conditions.

Cubic models are derived under variable stress conditions in order to capture coal permeability evolution behavior in the laboratory environment. The model proposed by Robertson and Christiansen [129] is one representative work. Compared to S&D model, the model by Robertson and Christiansen [129] predicts a reduction of the effect of gas sorption-induced strain on coal permeability change and can better match the experimental data. As cubic geometry is assumed in this model, for a given pore pressure, gas sorption-induced matrix swelling/

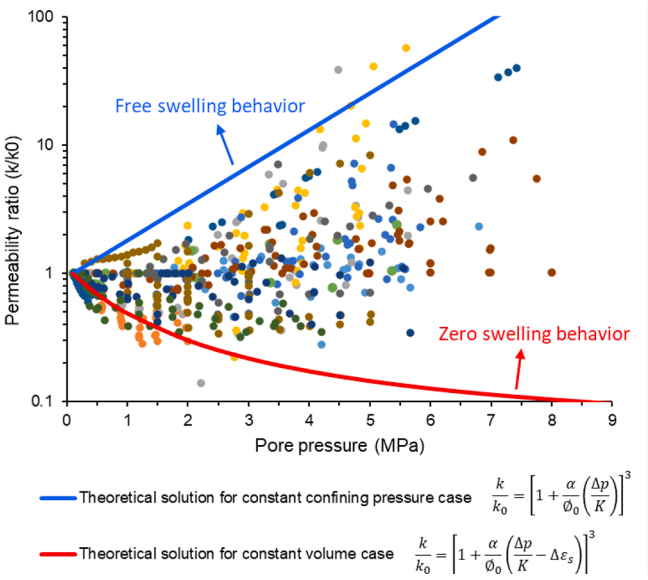

Fig. 9. Comparison of laboratory coal permeability data under CCP tests with poroelastic solutions (modified from Shi et al. [93]).

shrinkage will not contribute to coal permeability change under CCP condition [96,135,136]. However, this is not consistent with many laboratory observations that matrix swelling shows obvious impact on coal permeability when confining pressure remains unchanged [18,45,47]. The discrepancy between theoretical analysis and laboratory observation is attributed to the oversimplification of coal structure, i.e., the assumed through-going fracture system [136]. In fact, numerous inorganic minerals such as kaolinite, pyrite and illite exist in coal fractures [165-167]. These minerals can create rock bridges between adjacent matrix blocks. Considering the existence of rock bridges, fractures will be compressed during matrix swelling as they are weak and soft structures in coal. Meanwhile, rock bridges will prevent matrix swelling from completely closing the fractures. Therefore, fracture-matrix interaction occurs in coal during gas sorption. As a result, part of matrix swelling strain will contribute to fracture aperture change and the remaining will result in coal bulk deformation [137,169]. Unfortunately, both matchstick and cubic models ignore the existence of rock

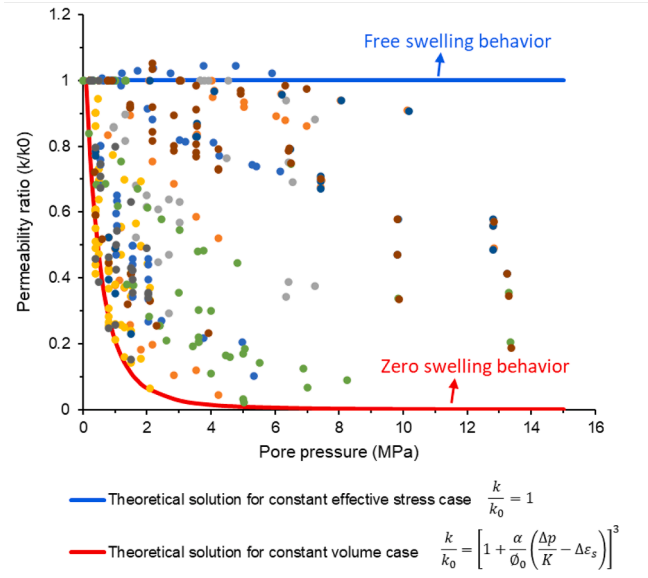

Fig. 10. Comparison of laboratory coal permeability data under CES tests with poroelastic solutions (modified from Shi et al. [93]).

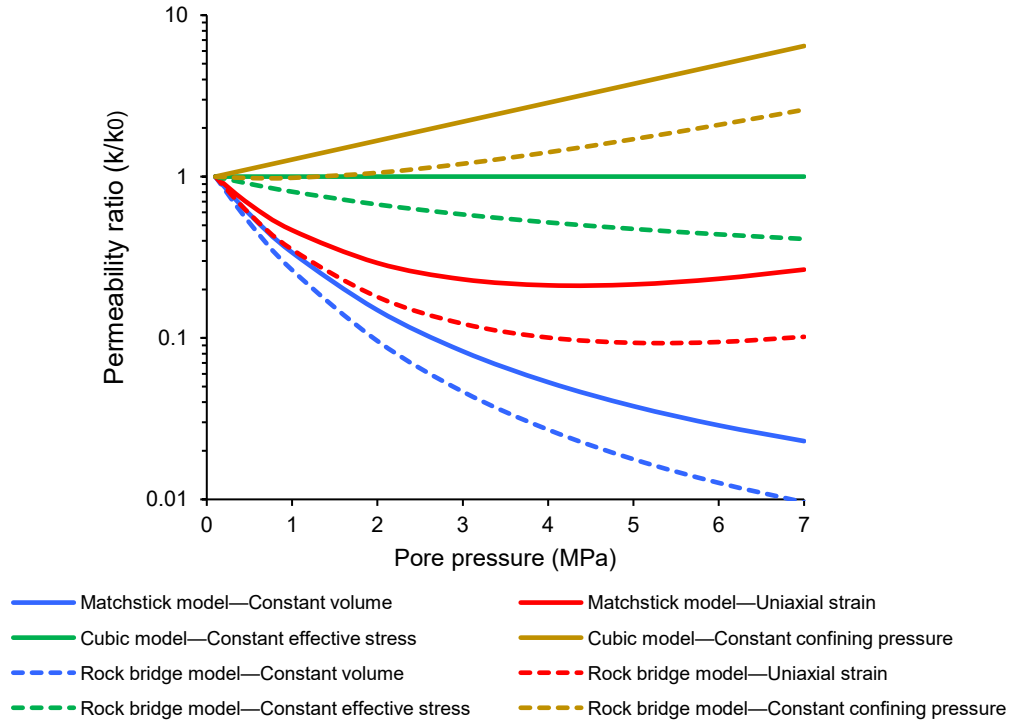

Fig. 11. Coal permeability curves generated by equilibrium permeability models under different boundary conditions.

bridge. This treatment leads to the inaccurate estimation of coal permeability.

Rock bridge models are developed to investigate the effect of gas sorption-induced fracture-matrix interaction on coal permeability change under variable stress conditions. The model proposed by Liu and Rutqvist [136] is the pioneering work in this stage. For the same coal mechanical and gas sorption parameters, the model by Liu and Rutqvist [136] can better match the reservoir permeability data from San Juan Basin and the laboratory data when compared with the model that doesn't consider fracture-matrix interaction.

According to the poroelastic theory, coal permeability should monotonically increase during gas injection tests under the CCP condition and remain unchanged during gas injection tests under the CES condition. Note that these poroelastic solutions are derived under the equilibrium assumption in which pressures in fracture and matrix systems are assumed to be equal. Similarly, when measuring coal permeability in the laboratory, it is also assumed that the equilibrium state is reached in the tested samples [93]. Hence, it can be hypothesized that the collected experimental data should match the poroelastic solutions if the equilibrium assumption was valid for both the poroelastic solutions and laboratory measurements. This hypothesis is checked through comparing experimental coal permeability data collected under CCP and CES conditions with the corresponding poroelastic solutions. As shown in Fig. 9 and Fig. 10, coal permeability ratio changes within a wide range. The poroelastic solutions for free swelling and zero swelling cases serve as the upper and lower envelopes of the randomly distributed coal permeability data, respectively. Thus, the experimental data collected under both CCP and CES conditions contradict with the theoretical solutions, which implies that coal permeability measurements were actually conducted under the non-equilibrium state. This phenomenon has been confirmed in recent laboratory experiments [56-60] and numerical studies [149-162]. According to these recent studies, the evolution of coal permeability under the non-equilibrium state can be divided into three or four distinct stages depending on how the boundary conditions are considered. The transition at different stages represents the evolution of coal permeability from initial equilibrium state, intermediate state, to the ultimate equilibrium state. In this work, we define coal permeability at the initial and ultimate equilibrium states as the equilibrium permeability and coal permeability at the intermediate state as the non-equilibrium permeability. By use of these definitions, the relation between experimental data and poroelastic solutions can be identified. The experimental data are collected as a mixture of equilibrium permeability and non-equilibrium permeability while the poroelastic solutions only represent the equilibrium permeability. The discrepancies between experimental data and poroelastic solutions require the removal of equilibrium assumption in theoretical models.

Here, it should be mentioned that although the pressure monitored during experiments may remain unchanged when recording coal permeability data, it is actually the stabilized fracture pressure being measured instead of the pressure of the whole coal sample. The matrix pressure may never reach the equilibrium state under the experimental conditions because the gas diffusion process in coal matrix will take a very long time to complete which may last from a few months to years [33,42,60,93].

In structure-based non-equilibrium models, the equilibrium assumption is removed and this represents a leap of knowledge from equilibrium to non-equilibrium theory. Applying the non– equilibrium models, the distribution rule of the "randomly" distributed coal permeability data as shown in Fig. 9 and Fig. 10 can be revealed as permeability models in this category are able to capture the complete evolution process of coal permeability from initial to ultimate equilibrium. The model proposed by Liu et al. [92] is the pioneering work in this category. Although some non-equilibrium coal permeability models have been proposed, the development of non-equilibrium theory is still in the initial stage and further research work needs to be done in this area.

Based on the above analysis, it can be concluded that coal permeability changes with both fracture pressure and time. Equilibrium permeability models including matchstick, cubic and rock bridge models establish the relation between coal permeability and fracture pressure. These poroelastic solutions use permeability curves to describe coal permeability change. In order to compare these equilibrium models, we

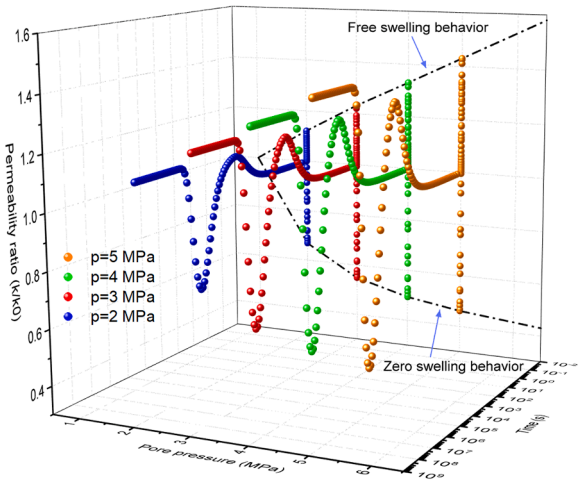

(a) Coal permeability map generated under the CCP condition

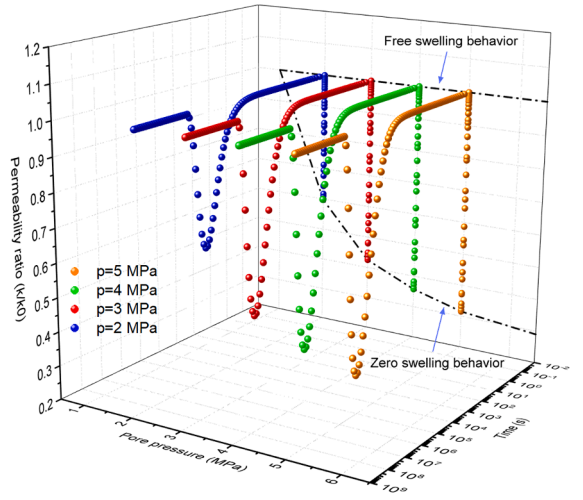

(b) Coal permeability map generated under the CES condition

Fig. 12. Coal permeability maps generated by the non-equilibrium model [163].

generate a series of coal permeability curves under a range of boundary conditions from stress-controlled to displacement-controlled, as shown in Fig. 11. The used parameters include $\varepsilon_L = 0.01$, $p_L = 4MPa$, $c_f = 0.1MPa^{-1}$ and $K = 2.5GPa$. These permeability curves are derived by a general coal permeability model which can represent permeability models in category 1. The derivation process of the general coal permeability model is given in Appendix A. From Fig. 11, it can be found that poroelastic solution under the CCP condition represents the upper envelope while poroelastic solution under the constant volume condition represents the lower envelope. Solutions under all other boundary conditions lie within the zone bounded by the two limiting envelopes. For further observation, the magnitude of permeability curve decreases when the role of rock bridge is considered.

Non-equilibrium models relate coal permeability with both fracture pressure and time. Applying the non-equilibrium model, permeability maps can be generated to describe coal permeability evolution. In comparison to conventional permeability curve, permeability map contains more information and captures the complete evolution process of coal permeability. Fig. 12 shows the permeability maps generated under the CCP and CES conditions. The parameters used for generating permeability maps are the same as above. It can be found that the variation of coal permeability is confined within two limiting envelopes. The upper envelope represents free swelling case while the lower envelope represents zero swelling case. Variation of coal permeability within the upper and lower envelopes is determined by the dynamics of fracture-matrix interaction. This explains why coal permeability ratio changes within a wide range in Fig. 9 and Fig. 10. Here, we take the gas injection case under the CCP condition as an example to illustrate how coal permeability evolves with time. Prior to gas injection, coal is under the equilibrium state and no interaction (gas diffusion, pore pressure and effective stress transfer) between fracture and matrix occurs in this stage. When gas injection starts, pressure in the fracture raises to injection pressure in a short time because of the relatively large permeability. As a result, a pressure difference is created between fracture and matrix which widens the fracture and increases coal permeability. Meanwhile, gas begins to diffuse into coal matrix through fracture wall under this pressure difference. When gas diffusion takes place in the vicinity of fracture, local swelling strain appears around the fracture which narrows the fracture and decreases coal permeability. With the continuation of gas diffusion, the invaded swelling zone enlarges and coal matrix swelling gradually transits from local swelling to global swelling which is characterized by the recovery of fracture aperture and coal permeability. When coal matrix is completely saturated with gas, the final equilibrium state is reached with pressures in fracture and matrix being the same. Under this condition, coal permeability stabilizes. The importance of each permeability evolution stage may be different and this depends on the permeability contrast between fracture and matrix. At present, permeability map is mainly used to explain experimental data. In the future, permeability map should serve as a tool for predicting coal permeability change under any boundary conditions. This requires the development of more robust non-equilibrium models.

5. Conclusions and recommendations

In this study, the state-of-the art status of coal permeability models is assessed through the critical review of coal permeability models available in the literature and its implications for further research are identified. Major conclusions are summarized as follows:

1) Coal permeability models can be classified into two major categories depending on how the internal structure of coal, boundary conditions and equilibrium state within the controlled volume are considered. In category 1, structured-based equilibrium models are developed. These equilibrium models can be further classified into matchstick models, cubic models and rock bridge models. Matchstick models are developed under the matchstick geometry, in-situ boundary conditions and equilibrium state. Cubic models are developed under the cubic geometry, variable stress conditions and equilibrium state. Rock bridge models are developed under the coal geometry containing rock bridges, variable stress conditions and equilibrium state. In category 2, structure-based non-equilibrium models are developed. These non-equilibrium models are developed under the coal geometry containing rock bridges, variable stress conditions, and non-equilibrium state.
2) The equilibrium models only serve as the upper and lower envelopes of experimental data while the non-equilibrium models can explain the data in-between. Further analysis indicates that if local equilibrium is achieved, gas pressure and its associated swelling strain distribute uniformly throughout the entire volume and that if not achieved, both pressure and swelling strain distribute non-uniformly. Therefore, the exclusion of equilibration process between fracture and matrix systems is the root cause of discrepancies between lab/field observations and model predictions. The history of model development indicates that the equilibration process within REV is particularly important for low permeable rocks like coal and shale because of the huge contrasts between fracture and matrix

properties and that future research work should integrate rock structure, boundary conditions and equilibration process into the permeability model. This inclusion of transient process within REV represents a leap of knowledge from equilibrium to non-equilibrium theory and opens up a new realm for unconventional gas reservoir modelling.

Declaration of Competing Interest

The authors declare that they have no known competing financial interests or personal relationships that could have appeared to influence the work reported in this paper.

Acknowledgements

This work is supported by the Australian Research Council under Grant DP200101293. The first author is also supported by the UWA-China Joint Scholarships (Grant No. 201906450050). These supports are gratefully acknowledged.

Appendix A

Both of the deformation of coal bulk and coal fracture consist of two parts. One part is caused by effective stress variation, and the other part is caused by gas sorption. Applying the volume balance principle, the volumetric strains of coal bulk and coal fracture are expressed as:

$$\frac{dV_b}{V_b} = -\frac{1}{K_b}(d\overline{\sigma} - \alpha dP) + d\varepsilon_s^b \tag{A1}$$

$$\frac{dV_f}{V_f} = -\frac{1}{K_f}(d\overline{\sigma} - \beta dP) + d\varepsilon_s^f \tag{A2}$$

where V_b and V_f are coal bulk volume and coal fracture volume, respectively. K_b and K_f are the bulk modulus of coal bulk and coal fracture, respectively. α and β are Biot coefficients. ε_s^b and ε_s^f are the gas sorption strains of coal bulk and coal fracture, respectively.

According to the definition of porosity, the following relations can be deduced:

$$\frac{dV_b}{V_b} = \frac{dV_m}{V_m} + \frac{d\varnothing_f}{1-\varnothing_f} \tag{A3}$$

$$\frac{dV_f}{V_f} = \frac{dV_m}{V_m} + \frac{d\varnothing_f}{\varnothing_f(1-\varnothing_f)} \tag{A4}$$

where V_m is the coal matrix volume, and $\varnothing_f$ is the fracture porosity.

Solving Eqs. (A1) to (A4), one can obtain:

$$\frac{d\varnothing_f}{\varnothing_f} = \left(\frac{1}{K} - \frac{1}{K_f}\right)(d\overline{\sigma} - dP) + \left(d\varepsilon_s^f - d\varepsilon_s^b\right) \tag{A5}$$

As K is commonly several orders of magnitude larger than K_f, $\frac{1}{K} - \frac{1}{K_f}$ can be reduced to $-\frac{1}{K_f}$. Through defining the relations $c_f = \frac{1}{K_f}$ and $f = \frac{d\varepsilon_s^f}{d\varepsilon_s^b}$, Eq. (A5) is rewritten into:

$$\frac{d\varnothing_f}{\varnothing_f} = -c_f(d\overline{\sigma} - dP) + (f-1)d\varepsilon_s^b \tag{A6}$$

Integrating Eq. (A6) yields the coal porosity ratio:

$$\frac{\varnothing_f}{\varnothing_{f0}} = exp\left\{-c_f[(\sigma - \sigma_0) - (p - p_0)] + (f-1)\Delta\varepsilon_s^b\right\} \tag{A7}$$

Applying the cubic law, coal permeability ratio can be obtained:

$$\frac{k_f}{k_{f0}} = exp\left\{-3c_f[(\sigma - \sigma_0) - (p - p_0)] + 3(f-1)\Delta\varepsilon_s^b\right\} \tag{A8}$$

Eq. (A8) is the general coal permeability model which can be transformed into different equilibrium models.

Applying the Hooke's law, the mean effective stress variation in coal under the uniaxial strain and constant vertical stress condition can be obtained:

$$\Delta\sigma_e = \frac{2E\Delta\varepsilon_s^b}{9(1-v)} - \frac{1+v}{3(1-v)}(p - p_0) \tag{A9}$$

where E and v are the elastic modulus and Poisson's ratio of coal, respectively.

Assuming $\varepsilon_s^f = \varepsilon_s^b$ and substituting Eq. (A9) into Eq. (A8), one can obtain the widely used C&B model [117] (matchstick model) under the uniaxial strain and constant vertical stress condition:

$\frac{k_f}{k_{f0}} = exp\left\{-c_f\left[\frac{2E\Delta\varepsilon_s^b}{3(1-v)} - \frac{1+v}{(1-v)}(p - p_0)\right]\right\}$(A10).

Under the constant volume condition, coal bulk strain is zero. Using Eq. (A1), one can obtain:

$d\varepsilon_s^b = \frac{1}{K_b}(d\overline{\sigma} - \alpha dP)$(A11).

Assuming $\alpha = 1$ gives:

$K_b d\varepsilon_s^b = d\overline{\sigma} - dP$(A12).

Assuming $\varepsilon_s^f = \varepsilon_s^b$ and substituting Eq. (A12) into Eq. (A6) yields:

$\frac{d\varnothing_f}{\varnothing_f} = -c_f K_b d\varepsilon_s^b$(A13).

Integrating Eq. (A13) gives coal porosity ratio under the constant volume condition:

$\frac{\varnothing_f}{\varnothing_{f0}} = exp\left(-c_f K_b \Delta\varepsilon_s^b\right)$(A14).

Applying the cubic law, matchstick model under the constant volume condition is obtained:

$\frac{k_f}{k_{f0}} = exp\left(-3c_f K_b \Delta\varepsilon_s^b\right)$(A15).

Assuming $\varepsilon_s^f = \varepsilon_s^b$, Eq. (A8) can be reduced to the permeability model proposed by Cao et al. [133] (cubic model):

$\frac{k_f}{k_{f0}} = exp\left\{-3c_f[(\sigma-\sigma_0)-(p-p_0)]\right\}$(A16).

Under the CCP condition, Eq. (A16) is reduced to:

$\frac{k_f}{k_{f0}} = exp\left[3c_f(p-p_0)\right]$(A17).

Under the CES condition, Eq. (A16) is reduced to:

$\frac{k_f}{k_{f0}} = 1$(A18).

Considering the existence of rock bridges in fracture, gas sorption-induced coal bulk strain and fracture strain will be different, i.e., $f \neq 1$. Substituting Eq. (A9) into Eq. (A8), one can obtain the rock bridge model under the uniaxial strain and constant vertical stress condition:

$\frac{k_f}{k_{f0}} = exp\left\{-c_f\left[\frac{2E\Delta\varepsilon_s^b}{3(1-\nu)} - \frac{1+\nu}{(1-\nu)}(p-p_0)\right] + 3(f-1)\Delta\varepsilon_s^b\right\}$(A19).

Under the constant volume condition, coal bulk strain is zero. Substituting Eq. (A12) into Eq. (A6) yields:

$\frac{d\varnothing_f}{\varnothing_f} = -c_f K_b d\varepsilon_s^b + (f-1)d\varepsilon_s^b$(A20).

Integrating Eq. (A20) gives coal porosity ratio under the constant volume condition:

$\frac{\varnothing_f}{\varnothing_{f0}} = exp\left\{-\left(c_f K_b - f + 1\right)\Delta\varepsilon_s^b\right\}$(A21).

Applying the cubic law, rock bridge model under the constant volume condition is obtained:

$\frac{k_f}{k_{f0}} = exp\left\{-3\left(c_f K_b - f + 1\right)\Delta\varepsilon_s^b\right\}$(A22).

The general coal permeability model in Eq. (A8) also represents the rock bridge model proposed by Jiang et al. [147]:

$\frac{k_f}{k_{f0}} = exp\left\{-3c_f[(\sigma-\sigma_0)-(p-p_0)] + 3(f-1)\Delta\varepsilon_s^b\right\}$(A23).

Under the CCP condition, Eq. (A23) is reduced to:

$\frac{k_f}{k_{f0}} = exp\left\{3c_f(p-p_0) + 3(f-1)\Delta\varepsilon_s^b\right\}$(A24).

Under the CES condition, Eq. (A23) is reduced to:

$\frac{k_f}{k_{f0}} = exp\left\{3(f-1)\Delta\varepsilon_s^b\right\}$(A25).

References

[1] Senthamaraikkannan G, Gates I, Prasad V. Development of a multiscale microbial kinetics coupled gas transport model for the simulation of biogenic coalbed methane production. Fuel 2016;167:188–98.

[2] Wang JG, Kabir A, Liu JS, Chen ZW. Effects of non-Darcy flow on the performance of coal seam gas wells. Int J Coal Geol 2012;93:62–74.

[3] Shi JQ, Durucan S. Drawdown induced changes in permeability of coalbeds: a new interpretation of the reservoir response to primary recovery. Transport Porous Med 2004;56:1–16.

[4] Clarkson CR, Bustin RM. Coalbed methane: current field-based evaluation methods. SPE Reserv Eval Eng 2011;14:60–75.

[5] Engler TW. A new approach to gas material balance in tight gas reservoirs. In: SPE Annual Technical Conference and Exhibition, Dallas, Texas, 2000.

[6] Bai M, Elsworth D. Coupled processes in subsurface deformation, flow and transport. ASCE Press; 2000.

[7] Elsworth D, Bai M. Flow-deformation response of dual porosity media. J Geotechnical Eng 1992;118:107–24.

[8] Wang SG, Elsworth D, Liu JS. A mechanistic model for permeability evolution in fractured sorbing media. J Geophys Res-Sol Ea 2012;117:B06205.

[9] Bai TH, Chen ZW, Aminossadati SM, Li N, Liu JS, Lu H. Dimensional analysis and prediction of coal fines generation under two-phase flow conditions. Fuel 2017; 194:460–79.

[10] Chen D, Pan ZJ, Liu JS, Connell LD. An improved relative permeability model for coal reservoirs. Int J Coal Geol 2013;109–110:45–57.

[11] Clarkson CR, Jordan CL, Gierhart RR, Seidle JP. Production data analysis of coalbed-methane wells. SPE Reserv Eval Eng 2008;11:311–25.

[12] Kissell FN, Edwards JC. Two-phase flow in coalbeds. Bur Mines Rep Invest 1975; 8066.

[13] Zhang JY, Feng QH, Zhang XM, Wang SM, Zhai YY. Relative permeability of coal: A review. Transport Porous Med 2015;106:563–94.

[14] Gray I. Reservoir engineering in coal seams: part 1—the physical process of gas storage and movement in coal seams. SPE Reserv Eng 1987;2:28–34.

[15] Ye DY, Liu GN, Gao F, Xu RG, Yue FT. A multi-field coupling model of gas flow in fractured coal seam. Adv Geo-Energy Res 2021;5(1):104–18.

[16] Connell LD. Coupled flow and geomechanical processes during gas production from coal seams. Int J Coal Geol 2009;79:18–28.

[17] Fang HH, Sang SX, Liu SQ. Numerical simulation of enhancing coalbed methane recovery by injecting CO2 with heat injection. Petrol Sci 2019;16:32–43.

[18] Pini R, Ottiger S, Burlini L, Storti G, Mazzotti M. CO2 storage through ECBM recovery: an experimental and modeling study. Energy Procedia 2009;1:1711–7.

[19] Niu QH, Cao LW, Sang SX, Wang W, Yuan W, Chang JF, et al. A small-scale experimental study of CO2 enhanced injectivity methods of the high-rank coal. Petrol Sci 2015;12:692–704.

[20] Zhang JF, Liu KY, Clennell MB, Dewhurst DN, Pan ZJ, Pervukhina M, et al. Molecular simulation studies of hydrocarbon and carbon dioxide adsorption on coal. Petrol Sci 2021;18:1427–40.

[21] Zarrouk SJ, Moore TA. Preliminary reservoir model of enhanced coalbed methane (ECBM) in a subbituminous coal seam, Huntly Coalfield. New Zealand Int J Coal Geol 2009;77:153–61.

[22] Chikatamarla L, Cui X, Bustin RM. Implications of volumetric swelling/shrinkage of coal in sequestration of acid gases. In: Proceedings of International Coalbed Methane Symposium, Tuscaloosa, Alabama, 2004.

[23] Flores RM. Coalbed methane: From hazard to resource. Int J Coal Geol 1998;35: 3–26.

[24] Yin GZ, Li MH, Wang JG, Xu J, Li WP. Mechanical behavior and permeability evolution of gas in filtrated coals during protective layer mining. Int J Rock Mech Min 2015;80:292–301.

[25] Li ZB, Wei GM, Liang R, Shi PP, Wen H, Zhou WH. LCO2-ECBM technology for preventing coal and gas outburst: Integrated effect of permeability improvement and gas displacement. Fuel 2021;285:119219.

[26] Chen DD, He WR, Xie SR, He FL, Zhang Q, Qin BB. Increased permeability and coal and gas outburst prevention using hydraulic flushing technology with cross-seam borehole. J Nat Gas Sci Eng 2020;73:103067.

[27] Dabbous MK, Reznik AA, Taber JJ, Fulton PF. The permeability of coal to gas and water. SPE J 1974;14:563–72.

[28] Rose RE, Foh SE. Liquid permeability of coal as a function of net stress. Pennsylvania: Pittsburgh; 1984.

[29] Seidle JP, Jeansonne MW, Erickson DJ. Application of matchstick geometry to stress dependent permeability in coals. In: SPE rocky mountain regional meeting, Casper, Wyoming, 1992.

[30] Chen ZW, Pan ZJ, Liu JS, Connell LD, Elsworth D. Effect of the effective stress coefficient and sorption-induced strain on the evolution of coal permeability: experimental observations. Int J Greenh Gas Con 2011;5:1284–93.

[31] Siriwardane H, Haljasmaa I, McLendon R, Irdi G, Soong Y, Bromhal G. Influence of carbon dioxide on coal permeability determined by pressure transient methods. Int J Coal Geol 2009;77:109–18.

[32] Somerton WH, Söylemezoglu IM, Dudley RC. Effect of stress on permeability of coal. Int J Rock Mech Min 1975;12:129–45.

[33] Guo R, Mannhardt K, Kantzas A. Laboratory investigation on the permeability of coal during primary and enhanced coalbed methane production. In: Canadian International Petroleum Conference, Calgary, Alberta, 2007.
[34] Harpalani S, Schraufnagel RA. Measurement of parameters impacting methane recovery from coal seams. Geotech Geol Eng 1990;8:369–84.
[35] Harpalani S, Zhao X. The unusual response of coal permeability to varying gas pressure and effective stress. In: Proceedings of the 30th US Symposium on Rock Mechanics (USRMS). Morgantown, 1989.
[36] Kumar H, Elsworth D, Liu J, Pone D, Mathews JP. Permeability evolution of propped artificial fractures in coal on injection of CO2. J Petrol Sci Eng 2015;133:695–704.
[37] Ranathunga AS, Perera SA, Gamage RP. An experimental study to investigate the temperature effect on permeability of victorian brown coal during CO2 sequestration. In: ISRM International Symposium-Proceedings of the 8th Asian Rock Mechanics Symposium, Sapporo, 2014.
[38] Robertson EP, Christiansen RL. Modeling permeability in coal using sorption-induced strain data. Idaho National Laboratory (INL) 2005.
[39] Wang SG, Elsworth D, Liu JS. Permeability evolution in fractured coal: the roles of fracture geometry and water-content. Int J Coal Geol 2011;87:13–25.
[40] Gensterblum Y, Ghanizadeh A, Krooss BM. Gas permeability measurements on Australian subbituminous coals: fluid dynamic and poroelastic aspects. J Nat Gas Sci Eng 2014;19:202–14.
[41] Meng J, Nie B, Zhao B, Ma Y. Study on law of raw coal seepage during loading process at different gas pressures. Min Sci Techno (In Chinese) 2015;25:31–5.
[42] Danesh NN, Chen Z, Connell LD, Kizil MS, Pan ZJ, Aminossadati SM. Characterisation of creep in coal and its impact on permeability: an experimental study. Int J Coal Geol 2017;173:200–11.
[43] Wang Y, Liu SM, Elsworth D. Laboratory investigations of gas flow behaviors in tight anthracite and evaluation of different pulse-decay methods on permeability estimation. Int J Coal Geol 2015;149:118–28.
[44] Harpalani S, Schraufnagel RA. Shrinkage of coal matrix with release of gas and its impact on permeability of coal. Fuel 1990;69:551–6.
[45] Harpalani S, Chen G. Influence of gas production induced volumetric strain on permeability of coal. Geotech Geol Eng 1997;15:303–25.
[46] Al-hawaree M. Geomechanics of CO2 sequestration in coalbed methane reservoirs. University of Alberta 1999.
[47] Pan ZJ, Connell LD, Camilleri M. Laboratory characterisation of coal reservoir permeability for primary and enhanced coalbed methane recovery. Int J Coal Geol 2010;82:252–61.
[48] Lin W, Tang GQ, Kovscek AR. Sorption-induced permeability change of coal during gas-injection processes. SPE Reserv Eval Eng 2008;11:792–802.
[49] Li J, Liu D, Yao Y, Cai Y, Chen Y. Evaluation and modeling of gas permeability changes in anthracite coals. Fuel 2013;111:606–12.
[50] Lin W, Kovscek AR. Gas sorption and the consequent volumetric and permeability change of coal I: experimental. Transport Porous Med 2014;105:371–89.
[51] Seomoon H, Lee M, Sung W. Analysis of sorption-induced permeability reduction considering gas diffusion phenomenon in coal seam reservoir. Transport Porous Med 2015;108:713–29.
[52] Li J, Liu D, Lu S, Yao Y, Xue H. Evaluation and modeling of the CO2 permeability variation by coupling effective pore size evolution in anthracite coal. Energ Fuel 2015;29:717–23.
[53] Anggara F, Sasaki K, Sugai Y. The correlation between coal swelling and permeability during CO2 sequestration: a case study using Kushiro low rank coals. Int J Coal Geol 2016;166:62–70.
[54] Meng Y, Li Z. Triaxial experiments on adsorption deformation and permeability of different sorbing gases in anthracite coal. J Nat Gas Sci Eng 2017;46:59–70.
[55] Feng R, Harpalani S, Pandey R. Evaluation of various pulse-decay laboratory permeability measurement techniques for highly stressed coals. Rock Mech Rock Eng 2017;50:297–308.
[56] Liu ZH, Liu JS, Pan PZ, Elsworth D, Wei MY, Shi R. Evolution and analysis of gas sorption-induced coal fracture strain data. Petrol Sci 2020;17:376–92.
[57] Shi R, Liu JS, Wang XM, Elsworth D, Liu ZH, Wei MY, et al. Experimental observations of heterogeneous strains inside a dual porosity sample under the influence of gas-sorption: A case study of fractured coal. Int J Coal Geol 2020;223:103450.
[58] Lin J, Ren T, Cheng YP, Nemcik J. Laboratory quantification of coal permeability reduction effect during carbon dioxide injection process. Process Saf Environ 2021;148:638–49.
[59] Wang CG, Zhang JD, Zang YX, Zhong RZ, Wang JG, Wu Y, et al. Time-dependent coal permeability: Impact of gas transport from coal cleats to matrices. J Nat Gas Sci Eng 2021;88:103806.
[60] Wei MY, Liu JS, Shi R, Elsworth D, Liu ZH. Long-term evolution of coal permeability under effective stresses gap between matrix and fracture during CO2 injection. Transport Porous Med 2019;130:969–83.
[61] Wold MB, Connell LD, Choi SK. The role of spatial variability in coal seam parameters on gas outburst behaviour during coal mining. Int J Coal Geol 2008;75:1–14.
[62] Clarkson CR, Bustin RM, Seidle JP. Production-data analysis of single-phase (gas) coalbed-methane wells. SPE Reserv Eval Eng 2007;10:312–31.
[63] Clarkson CR, Pan Z, Palmer ID, Harpalani S. Predicting sorption-induced strain and permeability increase with depletion for coalbed-methane reservoirs. In: SPE Annual Technical Conference and Exhibition, Denver, Colorado, 2008.
[64] Clarkson CR, Pan Z, Palmer ID, Harpalani S. Predicting sorption-induced strain and permeability increase with depletion for coalbed-methane reservoirs. SPE J 2010;15:152–9.
[65] Enever JRE, Hennig A. The relationship between permeability and effective stress for Australian coals and its implications with respect to coalbed methane exploration and reservoir modelling. In: International coalbed methane symposium, Tuscaloosa, 1997.
[66] Gierhart RR, Clarkson CR, Seidle JP. Spatial variation of San Juan basin Fruitland coalbed methane pressure dependent permeability: Magnitude and functional form. In: International Petroleum Technology Conference, Dubai, 2007.
[67] Mavor MJ, Vaughn JE. Increasing coal absolute permeability in the San Juan basin Fruitland formation. SPE Reserv Eval Eng 1998;1:201–6.
[68] McGovern M. Allison Unit CO2 flood: Project technical and economic review. In: SPE advanced technology workshop on enhanced coalbed methane recovery and CO2 sequestration, Denver, 2004. [69] Sparks DP, McLendon TH, Saulsberry JL, Lambert SW. The effects of stress on coalbed reservoir performance, BlackWarrior Basin, U.S.A. In: SPE annual technical conference and exhibition, Dallas, Texas, 1995.
[69] Young GBC, McElhiney JE, Paul GW, McBane RA. An analysis of fruitland coalbed methane production, Cedar Hill Field, Northern San Juan Basin. In: SPE Annual Technical Conference and Exhibition, Dallas, Texas, 1991.
[70] George Jr JK, Oudinot AY, McColpin GR, Liu N, Heath JE, Wells A, Young GB. CO2-ECBM/storage activities at the San Juan Basin's pump canyon test site. In: SPE Annual Technical Conference and Exhibition, New Orleans, Louisiana, 2009.
[71] Mavor MJ, Gunter WD, Robinson JR. Alberta multiwall micro-pilot testing for CBM properties, enhanced methane recovery and CO2 storage potential. In: SPE Annual Technical Conference and Exhibition, Houston, Texas, 2004.
[72] Oudinot AY, Koperna G, Philip ZG, Liu N, Heath JE, Wells A, Young GB, Wilson T. CO2 injection performance in the Fruitland coal fairway, San Juan Basin: results of a field pilot. In: SPE International Conference on CO2 Capture, Storage, and Utilization, San Diego, CA, USA, 2009.
[73] Reeves SR, Taillefert A, Pekot L, Clarkson C. The Allison unit CO2-ECBM pilot: a reservoir modeling study. Topical Report, DOE Contract No. DEFC26-00NT40924, 2003.
[74] Reeves S, Oudinot A. The Allison unit CO2-ECBM pilot—a reservoir and economic analysis. In: Proceedings of the International Coalbed Methane Symposium, Tuscaloosa, Alabama, 2005.
[75] Van Bergen F, Pagnier H, Krzystolik P. Field experiment of enhanced coalbed methane-CO2 in the upper Silesian basin of Poland. Environ Geosci 2006;13:201–24.
[76] Wong S, Law D, Deng X, Robinson J, Kadatz B, Gunter WD, et al. Enhanced coalbed methane and CO2 storage in anthracitic coals—micropilot test at South Qinshui, Shanxi. China Int J Greenh Gas Con 2007;1:215–22.
[77] Pan ZJ, Connell LD. Modelling permeability for coal reservoirs: A review of analytical models and testing data. Int J Coal Geol 2012;92:1–44.
[78] Xue S, Zheng CS, Kizil M, Jiang BY, Wang ZG, Tang MY, et al. Coal permeability models for enhancing performance of clean gas drainage: A review. J Petrol Sci Eng 2021;199:108283.
[79] Warren JE, Root PJ. The behavior of naturally fractured reservoirs. SPE J 1963;3:245–55.
[80] Wu Y, Liu JS, Elsworth D, Chen ZW, Connell L, Pan ZJ. Dual poroelastic response of a coal seam to CO2 injection. Int J Greenh Gas Con 2010;4:668–78.
[81] Wu Y, Liu JS, Elsworth D, Miao XX, Mao XB. Development of anisotropic permeability during coalbed methane production. J Nat Gas Sci Eng 2010;2:197–210.
[82] Lu M, Connell L. A statistical representation of the matrix-fracture transfer function for porous media. Transport Porous Med 2011;86:777–803.
[83] Van Golf-Racht TD. Fundamentals of Fractured Reservoir Engineering. Amsterdam: Elsevier; 1982.
[84] Liu SG, Tang SL, Yin SD. Coalbed methane recovery from multilateral horizontal wells in Southern Qinshui Basin. Adv Geo-Energy Res 2018;2(1):34–42.
[85] Palmer ID, Mavor M, Gunter B. Permeability changes in coal seams during production and injection. Tuscaloosa: University of Alabama; 2007.
[86] Cui X, Bustin RM, Chikatamarla L. Adsorption-induced coal swelling and stress: Implications for methane production and acid gas sequestration into coal seams. J Geophys Res-Sol Ea 2007;112:B10202.
[87] Day S, Fry R, Sakurovs R. Swelling of Australian coals in supercritical CO2. Int J Coal Geol 2008;74:41–52.
[88] Durucan S, Ahsanb M, Shi JQ. Matrix shrinkage and swelling characteristics of European coals. Energy Procedia 2009;1:3055–62.
[89] Palmer I, Reeves SR. Modeling changes of permeability in coal seams. Final Report, DOE Contract No. DE-FC26-00NT40924, 2007.
[90] Ritter D, Vinson D, Barnhart E, Akob DM, Fields MW, Cunningham AB, et al. Enhanced microbial coalbed methane generation: A review of research, commercial activity, and remaining challenges. Int J Coal Geol 2015;146:28–41.
[91] Liu JS, Wang JG, Chen ZW, Wang SG, Elsworth D, Jiang YD. Impact of transition from local swelling to macro swelling on the evolution of coal permeability. Int J Coal Geol 2011;88:31–40.
[92] Shi R, Liu JS, Wei MY, Elsworth D, Wang XM. Mechanistic analysis of coal permeability evolution data under stress-controlled conditions. Int J Rock Mech Min 2018;110:36–47.
[93] Koenig RA, Stubbs PB. Interference testing of a coalbed methane reservoir. In: SPE Unconventional Gas Technology Symposium, Louisville, Kentucky, 1986.
[94] Gash BW, Richard FV, Potter G, Corgan JM. The effects of cleat orientation and confining pressure on cleat porosity, permeability and relative permeability in coal. In: SPWLA/SCA Symposium, Oklahoma City, 1992.
[95] Liu JS, Chen ZW, Elsworth D, Qu HY, Chen D. Interactions of multiple processes during CBM extraction: a critical review. Int J Coal Geol 2011;87:175–89.

[96] Clavard JB, Maineult A, Zamora M, Rasolofosaon P, Schlitter C. Permeability anisotropy and its relations with porous medium structure. J Geophys Res 2008; 113(B1):B01202.
[97] Xu X, Sarmadivaleh M, Li C, Xie B, Iglauer S. Experimental study on physical structure properties and anisotropic cleat permeability estimation on coal cores from China. J Nat Gas Sci Eng 2016;35(Part A):131-143.
[98] Fu B, Liu G, Liu Y, Cheng S, Qi C, Sun R. Coal quality characterization and its relationship with geological process of the Early Permian Huainan coal deposits, southern North China. J Geochem Explor 2016;166:33–44.
[99] Heriawan MN, Koike K. Identifying spatial heterogeneity of coal resource quality in a multilayer coal deposit by multivariate geostatistics. Int J Coal Geol 2008;73 (3–4):307–30.
[100] Tan YL, Pan ZJ, Liu JS, Zhou FB, Connell LD, Sun WJ, et al. Experimental study of impact of anisotropy and heterogeneity on gas flow in coal. Part II: Permeability Fuel 2018;230:397–409.
[101] Danesh NN, Chen ZW, Aminossadati SM, Kizil MS, Pan ZJ, Connell LD. Impact of creep on the evolution of coal permeability and gas drainage performance. J Nat Gas Sci Eng 2016;33:469–82.
[102] Schatzel SJ, Karacan CO, Dougherty H, Goodman GVR. An analysis of reservoir conditions and responses in longwall panel overburden during mining and its effect on gob gas well performance. Eng Geol 2012;127:65–74.
[103] Xue Y, Gao F, Liu XG. Effect of damage evolution of coal on permeability variation and analysis of gas outburst hazard with coal mining. Nat Hazards 2015;79: 999–1013.
[104] Palmer I, Mansoori J. How permeability depends on stress and pore pressure in coalbeds: a new model. SPE Reserv Eval Eng 1998;1:539–44.
[105] Wang CG, Feng JL, Liu JS, Wei MY, Wang CS, Gong B. Direct observation of coal-gas interactions under thermal and mechanical loadings. Int J Coal Geol 2014; 131:274–87.
[106] Zhu WC, Wei CH, Liu J, Qu HY, Elsworth D. A model of coal-gas interaction under variable temperatures. Int J Coal Geol 2011;86:213–21.
[107] Shang X, Wang JG, Zhang Z, Gao F. A three-parameter permeability model for the cracking process of fractured rocks under temperature change and external loading. Int J Rock Mech Min 2019;123:104106.
[108] Bai TH, Chen ZW, Aminossadati SM, Pan ZJ, Liu JS, Li L. Characterization of coal fines generation: A micro-scale investigation. J Nat Gas Sci Eng 2015;27:862–75.
[109] Bai TH, Chen ZW, Aminossadati SM, Rufford TE, Li L. Experimental investigation on the impact of coal fines generation and migration on coal permeability. J Petrol Sci Eng 2017;159:257–66.
[110] Harpalani S, Chen G. Estimation of changes in fracture porosity of coal with gas emission. Fuel 1995;74:1491–8.
[111] Ma Q, Harpalani S, Liu SM. A simplified permeability model for coalbed methane reservoirs based on matchstick strain and constant volume theory. Int J Coal Geol 2011;85:43–8.
[112] Massarotto P, Golding SD, Rudolph V. Constant volume CBM reservoirs: An important principle. In: International Coalbed Methane Symposium, Tuscaloosa, Alabama, 2009.
[113] Reiss LH. The reservoir engineering aspects of fractured formations. Houston: Gulf Publishing Co.; 1980.
[114] McKee C, Bumb A, Koenig R. Stress-dependent permeability and porosity of coal and other geologic formations. SPE Form Eval 1988;3:81–91.
[115] Gilman A, Beckie R. Flow of coal-bed methane to a gallery. Transport Porous Med 2000;41:1–16.
[116] Cui XJ, Bustin RM. Volumetric strain associated with methane desorption and its impact on coalbed gas production from deep coal seams. AAPG Bull 2005;89: 1181–202.
[117] Levine JR. Model study of the influence of matrix shrinkage on absolute permeability of coal bed reservoirs. Geological Society, London, Special Publications 1996;109:197–212.
[118] Seidle JR, Huitt LG. Experimental measurement of coal matrix shrinkage due to gas desorption and implications for cleat permeability increases. In: International Meeting on Petroleum Engineering, Beijing, China, 1995.
[119] Sawyer WK, Zuber MD, Kuuskraa VA, Horner DM. Using reservoir simulation and field data to define mechanisms controlling coalbed methane production. In: Proceedings of the 1987 Coalbed Methane Symposium, Alabama, 1987.
[120] Sawyer WK, Paul GW, Schraufnagel RA. Development and application of a 3D coalbed simulator. In: International Technical Meeting Hosted Jointly by the Petroleum Society of CIM and the Society of Petroleum Engineers, Calgary, Alberta, Canada. 1990.
[121] Pekot LJ, Reeves SR. Modeling coal matrix shrinkage and differential swelling with CO2 injection for enhanced coalbed methane recovery and carbon sequestration applications. Topical report, Contract No. DE-FC26-00NT40924, U. S. DOE, Washington, DC. 2002.
[122] Pekot LJ, Reeves SR. Modeling the effects of matrix shrinkage and differential swelling on coalbed methane recovery and carbon sequestration. Tuscaloosa: University of Alabama; 2003.
[123] Palmer I, Mansoori J. How permeability depends on stress and pore pressure in coalbeds: a new model. In: SPE Annual Technical Conference and Exhibition, Denver, Colorado. 1996.
[124] Gu F, Chalaturnyk JJ. Analysis of coalbed methane production by reservoir and geomechanical coupling simulation. J Can Petrol Technol 2005;44:33–42.
[125] Gu F, Chalaturnyk R. Permeability and porosity models considering anisotropy and discontinuity of coalbeds and application in coupled simulation. J Petrol Sci Eng 2010;74:113–31.
[126] Pan ZJ, Connell LD. Modelling of anisotropic coal swelling and its impact on permeability behaviour for primary and enhanced coalbed methane recovery. Int J Coal Geol 2011;85:257–67.
[127] Jaeger GC, Cook NGW. Fundamentals of Rock Mechanics. London: Chapman and Hall Ltd and Science Paperbacks; 1969.
[128] Robertson EP, Christiansen RL. A permeability model for coal and other fractured, sorptive-elastic media. SPE J 2008;13:314–24.
[129] Robertson EP, Christiansen RL. A permeability model for coal and other fractured, sorptive-elastic media. In: SPE Eastern Regional Meeting, Canton, Ohio, USA, 2006.
[130] Zhang HB, Liu JS, Elsworth D. How sorption-induced matrix deformation affects gas flow in coal seams: a new FE model. Int J Rock Mech Min 2008;45:1226–36.
[131] Liu JS, Chen ZW, Elsworth D, Miao XX, Mao XB. Evolution of coal permeability from stress-controlled to displacement-controlled swelling conditions. Fuel 2011; 90:2987–97.
[132] Cao P, Liu JS, Leong YK. General gas permeability model for porous media: Bridging the gaps between conventional and unconventional natural gas reservoirs. Energ Fuel 2016;30:5492–505.
[133] Wang GX, Massarotto P, Rudolph V. An improved permeability model of coal for coalbed methane recovery and CO2 geosequestration. Int J Coal Geol 2009;77: 127–36.
[134] Connell LD, Lu M, Pan ZJ. An analytical coal permeability model for tri-axial strain and stress conditions. Int J Coal Geol 2010;84:103–14.
[135] Liu HH, Rutqvist J. A new coal-permeability model: internal swelling stress and fracture-matrix interaction. Transport Porous Med 2010;82:157–71.
[136] Chen ZW, Liu JS, Pan ZJ, Connell LD, Elsworth D. Influence of the effective stress coefficient and sorption-induced strain on the evolution of coal permeability: Model development and analysis. Int J Greenh Gas Con 2012;8:101–10.
[137] Guo PK, Cheng YP, Jin K, Li W, Tu QY, Liu HY. Impact of effective stress and matrix deformation on the coal fracture permeability. Transport Porous Med 2014;103:99–115.
[138] Wang K, Zang J, Wang G, Zhou A. Anisotropic permeability evolution of coal with effective stress variation and gas sorption: model development and analysis. Int J Coal Geol 2014;130:53–65.
[139] Lu S, Cheng Y, Li W. Model development and analysis of the evolution of coal permeability under different boundary conditions. J Nat Gas Sci Eng 2016;31: 129–38.
[140] Liu T, Lin B, Yang W. Impact of matrix-fracture interactions on coal permeability: model development and analysis. Fuel 2017;207:522–32.
[141] Yang X, Zhang HB, Wu WB, Gong ZH, Yuan WF, Feng XQ, et al. Gas migration in the reservoirs of ultra-low porosity and permeability based on an improved apparent permeability model. J Petrol Sci Eng 2020;185:106614.
[142] Zhou HW, Zhang L, Wang XY, Rong TL, Wang LJ. Effects of matrix-fracture interaction and creep deformation on permeability evolution of deep coal. Int J Rock Mech Min 2020;127:104236.
[143] Shi Y, Lin BQ, Liu T, Zhao Y, Hao ZY. Synergistic ECBM extraction technology and engineering application based on hydraulic flushing combing gas injection displacement in low permeability coal seams. Fuel 2022;318:123688.
[144] Li JH, Li BB, Cheng QY, Gao Z. Characterization of anisotropic coal permeability with the effect of sorption-induced deformation and stress. Fuel 2022;309: 122089.
[145] Peng Y, Liu JS, Pan ZJ, Connell LD, Chen ZW, Qu HY. Impact of coal matrix strains on the evolution of permeability. Fuel 2017;189:270–83.
[146] Jiang CZ, Zhao ZF, Zhang XW, Liu JS, Elsworth D, Cui GL. Controlling effects of differential swelling index on evolution of coal permeability. J Rock Mech Geotech 2020;12:461–72.
[147] Liu JS, Chen ZW, Elsworth D, Miao XX, Mao XB. Evaluation of stress-controlled coal swelling processes. Int J Coal Geol 2010;83:446–55.
[148] Chen ZW, Liu JS, Elsworth D, Pan ZJ, Wang SG. Roles of coal heterogeneity on evolution of coal permeability under unconstrained boundary conditions. J Nat Gas Sci Eng 2013;15:38–52.
[149] Qu HY, Liu JS, Chen ZW, Wang JG, Pan ZJ, Connell L, et al. Complex evolution of coal permeability during CO2 injection under variable temperatures. Int J Greenh Gas Con 2012;9:281–93.
[150] Qu HY, Liu JS, Pan ZJ, Connell L. Impact of matrix swelling area propagation on the evolution of coal permeability under coupled multiple processes. J Nat Gas Sci Eng 2014;18:451–66.
[151] Liu XX, Sheng JC, Liu JS, Hu YJ. Evolution of coal permeability during gas injection-From initial to ultimate equilibrium. Energies 2018;11:2800.
[152] Wei MY, Liu JS, Elsworth D, Li SJ, Zhou FB. Influence of gas adsorption induced non-uniform deformation on the evolution of coal permeability. Int J Rock Mech Min 2019;114:71–8.
[153] Peng Y, Liu JS, Wei MY, Pan ZJ, Connell LD. Why coal permeability changes under free swellings: New insights. Int J Coal Geol 2014;133:35–46.
[154] Zeng J, Liu JS, Li W, Tian JW, Leong YK, Elsworth D, Guo JC. Impact of swelling area expansion from the fracture wall into the matrix on the evolution of coal permeability. In: 5th ISRM Young Scholars' Symposium on Rock Mechanics and International Symposium on Rock Engineering for Innovative Future, Okinawa, Japan, 2019.
[155] Zeng J, Liu JS, Li W, Tian JW, Leong YK, Elsworth D, et al. Effects of heterogeneous local swelling and multiple pore types on coal and shale permeability evolution. In: SPE Europec, Virtual 2020.
[156] Zeng J, Liu JS, Li W, Guo JC. A process-based coal swelling model: Bridging the gaps between localized swelling and bulk swelling. Fuel 2021;293:120360.
[157] Liu XX, Sheng JC, Ma CX, Liu JS, Gao HC. Complete coal permeability models from initial to ultimate equilibrium. Fuel 2020;271:117612.

[158] Peng Y, Liu JS, Zhu WC, Pan ZJ, Connell L. Benchmark assessment of coal permeability models on the accuracy of permeability prediction. Fuel 2014;132:194–203.
[159] Zhu WC, Liu LY, Liu JS, Wei CH, Peng Y. Impact of gas adsorption-induced coal damage on the evolution of coal permeability. Int J Rock Mech Min 2018;101:89–97.
[160] Zhang SW, Liu JS, Wei MY, Elsworth D. Coal permeability maps under the influence of multiple coupled processes. Int J Coal Geol 2018;187:71–82.
[161] Wei MY, Liu JS, Elsworth D, Liu YK, Zeng J, He ZH. Impact of equilibration time lag between matrix and fractures on the evolution of coal permeability. Fuel 2021;290:120029.
[162] Huang YF, Liu JS, Elsworth D, Leong YK. A transient dual porosity/permeability model for coal multiphysics. Geomech Geophys Geo-energ Geo-resour 2022;8:40.
[163] Palmer I. Permeability changes in coal: Analytical modeling. Int J Coal Geol 2009;77:119–26.
[164] Karacan CO. Swelling-induced volumetric strains internal to a stressed coal associated with CO2 sorption. Int J Coal Geol 2007;72:209–20.
[165] Dawson GKW, Golding SD, Esterle JS, Massarotto P. Occurrence of minerals within fractures and matrix of selected Bowen and Ruhr Basin coals. Int J Coal Geol 2012;94:150–66.
[166] Wei MY, Liu JS, Liu YK, Liu ZH, Elsworth D. Effect of adsorption-induced matrix swelling on coal permeability evolution of micro-fracture with the real geometry. Petrol Sci 2021;18:1143–52.
[167] Zang J, Wang K, Zhao YX. Evaluation of gas sorption-induced internal swelling in coal. Fuel 2015;143:165–72.